



Published in final edited form as:

J Med Chem. 2020 May 14; 63(9): 4716–4731. doi:10.1021/acs.jmedchem.9b02164.

Discovery, Structure-Activity Relationship and Biological Activity of Histone-Competitive Inhibitors of Histone Acetyltransferases P300/CBP

Fangrui Wu^{1,§}, Yuanda Hua^{1,§}, Salma Kaochar^{2,3}, Shenyou Nie¹, Yi-Lun Lin¹, Yuan Yao¹, Jingyu Wu¹, Xiaowei Wu¹, Xiaoyong Fu⁴, Rachel Schiff^{2,4,5}, Christel M. Davis⁶, Matthew Robertson³, Erik A. Ehli⁶, Cristian Coarfa³, Nicholas Mitsiades^{2,3}, Yongcheng Song^{*,1,3}

¹Department of Pharmacology & Chemical Biology, Baylor College of Medicine, 1 Baylor Plaza, Houston, TX 77030, USA.

²Department of Medicine, Baylor College of Medicine, 1 Baylor Plaza, Houston, TX 77030, USA.

³Dan L. Duncan Cancer Center, Baylor College of Medicine, 1 Baylor Plaza, Houston, TX 77030, USA.

⁴Department of Molecular & Cellular Biology, Baylor College of Medicine, 1 Baylor Plaza, Houston, TX 77030, USA.

⁵Lester and Sue Smith Breast Center, Baylor College of Medicine, 1 Baylor Plaza, Houston, TX 77030, USA.

⁶Avera Institute for Human Genetics, Sioux Falls, SD 57108, USA.

Abstract

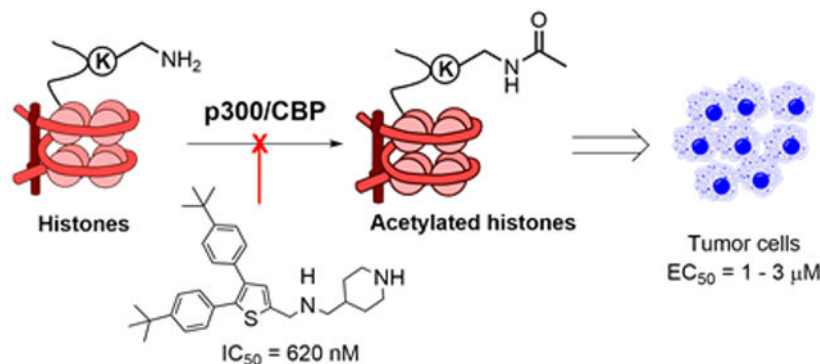
Histone acetyltransferase (HAT) p300 and its paralog CBP acetylate histone lysine sidechains and play critical roles in regulating gene transcription. The HAT domain of p300/CBP is a potential drug target for cancer. Through compound screening and medicinal chemistry, novel inhibitors of p300/CBP HAT with their IC₅₀s as low as 620 nM were discovered. The most potent inhibitor is competitive against histone substrates and exhibits a high selectivity for p300/CBP. It inhibited cellular acetylation and had strong activity with EC₅₀ of 1-3 μM against proliferation of several tumor cell lines. Gene expression profiling in estrogen receptor (ER)-positive breast cancer MCF-7 cells showed that inhibitor treatment recapitulated siRNA-mediated p300 knockdown, inhibited ER-mediated gene transcription, and suppressed expression of numerous cancer-related gene signatures. These results demonstrate that the inhibitor is not only a useful probe for biological studies of p300/CBP HAT, but also a pharmacological lead for further drug development targeting cancer.

* **CORRESPONDING AUTHOR FOOTNOTE:** To whom correspondence should be addressed. Address: Department of Pharmacology & Chemical Biology, Baylor College of Medicine, 1 Baylor Plaza, Houston, TX 77030. Tel: 713-798-7415. ysong@bcm.edu.

§ These authors contributed equally.

Supporting Information Available. Chart S1-S3, Figure S1-S4, representative HPLC traces and ¹H and ¹³C NMR spectra for compound **12** and PDB file for docking models. This material and Molecular Formula Strings for all compounds are available free of charge via the Internet at <http://pubs.acs.org>.

Graphical Abstract



Keywords

Histone acetyltransferase; p300/CBP; small-molecule inhibitor; Gene expression profiling; cancer therapy

INTRODUCTION

Histone acetylation is one of the most important post-translational modifications. Acetylation of the sidechain amino group of a histone lysine residue neutralizes its positive charge (under physiological pH) and renders a more open DNA conformation to facilitate binding of transcription factors as well as other proteins for gene transcription, DNA replication and repair^{1, 2}. In addition, acetylated lysine can be recognized by a number of proteins (such as bromodomain-containing proteins) and serve as an anchor point in chromatin to form a transcription complex that regulates gene expression^{3, 4}.

Human p300 (E1A binding protein p300) and its paralog CBP [CREB (cAMP-response element binding protein) binding protein] are large proteins with ~2,400 amino acids⁵⁻⁷, containing multiple structured domains including cysteine-histidine rich 1 (CH1), CREB-binding KIX, Bromodomain, histone acetyltransferase (HAT), CH3, and steroid receptor coactivator interaction (SID) domains. These structured domains, which share a high homology between p300 and CBP, are connected with less conserved intrinsically disordered regions (IDR). The CH1, KIX, CH3 and SID domains as well as IDR of p300/CBP are transactivation domains, which interact with a number of transcription factors (e.g., CREB, p53 and HIF-1) and transcription coactivators (e.g., steroid receptor coactivators)⁸⁻¹⁰. Biologically, p300/CBP not only acetylates a lysine residue of histone (e.g., histone H3 lysine 27, or H3K27) and certain transcription factors (e.g., p53 and c-Myc)^{7, 11, 12}, it also serves as a hub protein to link and stabilize a transcription complex.

Previous studies have shown that HAT activity of p300/CBP is essential for many transcription factor-mediated gene transcription programs. For example, estrogen receptor (ER) or androgen receptor (AR) mediated gene transcription pathway is of importance in female or male development as well as in breast or prostate cancer, respectively. HAT activity of p300 has been found to be required for ER- or AR-mediated gene expression

8, 10, 13. In addition, HAT of p300/CBP is a potential drug target for cancer therapy. Although there have been debates on whether p300/CBP alone is a tumor suppressor or an oncogene, convincing evidence has shown that p300/CBP HAT is essential for breast and prostate cancer as well as other cancers with p300 overexpression or harboring a p300/CBP fusion oncogene^{7, 14, 15}.

To date, several chemotypes of p300/CBP HAT inhibitors have been reported (Figure 1)^{6, 7}. However, except for recently disclosed compound A-485¹⁶, other compounds are not drug-like probes for cellular or in vivo studies. Lys-CoA and its analogs are not cell-permeable^{17, 18}. Compounds C646¹⁹, L002²⁰ and Cpd-2c²¹ contain a “PAINS” (pan-assay interfering compound)²² or related structure, which are unfavorable for drug development or cell biology. A-485 is a potent inhibitor of p300/CBP HAT, which is competitive against the enzyme cofactor acetyl coenzyme A (Ac-CoA)¹⁶. It showed strong activity against proliferation of several cancer cells. Nevertheless, given the low success rate in drug discovery, more chemotypes of p300 HAT inhibitors are needed. Here, we report discovery, structure activity relationships (SAR), biochemical and biological activities of a novel series of inhibitors of p300/CBP HAT that are competitive against the histone substrate.

RESULTS

Inhibitor discovery.

A biochemical assay to determine the activity and inhibition of recombinant HAT domain of human p300 was developed, using the substrate histone H3 (1-21) peptide and the ³H-labeled cofactor Ac-CoA. We screened our proprietary compound library containing ~300 compounds, which were synthesized for SAR studies of lysine specific demethylase 1 (LSD1)²³ whose substrate is methylated histone H3 lysine 4 (H3K4). The rationale is that since the peptide sequence of H3K4 (ARTKQ) is similar to those of p300 HAT's substrate H3K27 (AARKS), there is a higher likelihood to find an inhibitor from the LSD1 targeting compounds. The compound screen led to the discovery of thiophene-2-carbamide compound **1** (Table 1) that inhibited p300 HAT with an IC₅₀ (concentration at which the enzyme activity is inhibited by 50%) value of 8.6 μM.

Synthesis.

Given its seemingly drug-like structure, more derivatives of compound **1** were synthesized and tested for their activities against p300 HAT. General methods for synthesis of compounds **1-40** for SAR studies are shown in Scheme 1.

Synthesis of thiophene-2-carbamide compounds **1-9** was started from a reaction between 4,5-dibromo-thiophene-2-carboxylic acid (**41**) and 1-*tert*-butyloxycarbonyl (BOC) protected 4-(aminomethyl)piperidine, together with amide bond forming reagents 1-ethyl-3-(3-dimethylaminopropyl)carbodiimide (EDC) and 1-hydroxybenzotriazole. The 5- and 4-Br groups of the thiophene-2-carbamide compounds (**42**) can undergo two successive Suzuki coupling reactions with different aryl boronic acids with a high selectivity²⁴: 5-Br was reacted first at a lower temperature of 80 °C, followed by 4-Br at 100 °C, to give compound **43**. Removal of the BOC protecting group using HCl produced the target compounds **1-9**.

Synthesis of 2-aminomethylthiophene series of compounds **10-12** and **14-32** was started from 4,5-dibromo-thiophene-2-carbaldehyde (**44**, X = S), in which the 2-CHO group was reduced to an alcohol, followed by conversion to a -CH₂Cl group by treatment with cyanuric chloride in DMF. The -Cl of the product **45** was next substituted with 4-(aminomethyl)-1-BOC-piperidine or other amine analogs. The resulting 2-substituted 4,5-dibromo-thiophene compound **46** was subjected to two selective Suzuki coupling reactions to produce, upon deprotection of BOC, the target 2-aminomethylthiophene series of compounds.

Furan-containing inhibitors **34** and **35** were prepared similarly from 4,5-dibromo-furan-2-carbaldehyde (**44**, X = O). All thiazole compounds were synthesized from 4-bromothiazole-2-carbaldehyde (**48**), which was treated with N-bromosuccinimide to produce di-Br compound **49**. The aldehyde group of **48** and **49** was reduced and converted to a -CH₂Cl group in compound **50**, which was substituted with 1-BOC-4-(aminomethyl)piperidine followed by Suzuki coupling reactions to give, after deprotection, compounds **37** and **38**. Oxidation of **48** (or **49**) produced thiazole-2-carboxylic acid **51**, which was reacted with 1-BOC-4-(aminomethyl)piperidine followed by Suzuki coupling reactions to afford thiazole compound **39** (or **36**). For the synthesis of the pyrazine compound **40**, di-4-bromobenzil (**52**) was refluxed with 2,3-diaminopropanoic acid in methanol to give 5,6-di-(4-bromophenyl)pyrazine-2-carboxylic acid (**53**), whose -CO₂H group was acylated, reduced (with NaBH₄) to -CH₂OH, and converted to -CH₂Cl (**54**). A substitution reaction with 4-(aminomethyl)-1-BOC-piperidine followed by Suzuki coupling reactions produced compound **55**, which was treated with HCl to give compound **40**.

Structure-activity relationship.

The structures and inhibitory activities of compounds **1-32** are shown in Table 1 and Supporting Information Chart S1-3 and Figure S1. Compound **1**, having 4,5-di-substituted *tert*-butyl groups as well as a piperidine-containing amide group, had a moderate IC₅₀ of 8.6 μM. Compound **2** with 4,5-di-substituted furan-3-yl groups was found to have significantly enhanced inhibitory activity with an IC₅₀ of 1.6 μM, while compound **3** with two 4-methoxybiphenyl substituents showed slightly reduced inhibitory activity (IC₅₀ = 2.8 μM). Compound **4** bearing a mixed *tert*-butyl and furanyl group also exhibited a compromised activity (IC₅₀ = 7.4 μM). Compound **5** with a polar 4-aminomethylphenyl substituent rendered little activity change (IC₅₀ = 10 μM). However, compound **6** with a piperidine-containing 4-substituent, which is less polar as compared to the polar primary amine in **5**, showed an improved activity (IC₅₀ = 1.6 μM). Compound **7** having a piperazine group was found to be almost inactive at 10 μM, showing an additional amino group (as compared to **6**) is likely disfavored. Compounds **8** and **9** with no substituents in their 4-aromatic rings were found to have modest activity, inhibiting p300-HAT by ~30% at 10 μM, suggesting a substituent (e.g., furan-3-yl in **4**) at this position is favorable.

Next, activity optimization of the 2-carboxamide sidechain was performed for compounds **10-21** (Table 1 and Chart S2). The first attempt was to replace the amide sidechain (in e.g., **1** and **2**) with a piperidin-4-yl-methylaminomethyl group in compounds **10-12**. While removal of the carbonyl group reduces the activity of compound **10** (IC₅₀ = 7.4 μM) by ~50% (as compared to **3**), compound **11** with an IC₅₀ of 1.7 μM exhibited a comparable activity to that

of **2**. Of interest is that compound **12** showed a potent activity against p300-HAT with an IC_{50} of 620 nM, which is $\sim 13\times$ more active than its amide analog **1**. Changing the -NH- linkage (in **10-12**) to an -O- in compound **13** resulted in a complete loss of inhibitory activity, suggesting the -NH- (which is protonated at physiological pH) could be a key hydrogen bond donor. Compounds **14** and **15**, whose 2-substituents are one -CH₂- shorter and longer than that of **12**, respectively, were found to possess ~ 8 - and 3-fold activity reduction (IC_{50} = 5.0 and 2.2 μM). Compounds **16** and **17**, which carry a linear, ω -amino-propyl and -hexyl side chain, respectively, are also strong inhibitors with IC_{50} values of 3.0 and 1.4 μM . Loss of activity was found for compounds **18** and **19** bearing a 2-substituent of piperazin-1-ylmethyl and morpholin-4-ylmethyl group, showing shorter cyclic 2-substituents are disfavored. Moreover, methylation and formylation of the middle -NH- group (in compound **12**) produced compounds **20** and **21**, respectively, which were found to have less inhibitory activities with IC_{50} values of 4.4 and 7.0 μM . These results suggest an -NH- or -CONH- linkage, which might be a hydrogen bond donor, is of importance to the inhibition.

Compounds **22-32** (Table 1 and Chart S3) were synthesized to evaluate effects of varying 4- and/or 5-substituents of the most potent inhibitor **12**. Replacing the *tert*-butyl with isopropyl groups in **22** (IC_{50} = 5.4 μM) resulted in $\sim 8x$ activity reduction, suggesting a bulkier group is favorable for the 4- and 5-positions. Loss of activity for compound **23** with two *n*-butyl groups at these positions showed that long alkyl substituents are disfavored. Changing the 4-substituent to a furan-3-yl group in compound **24** (IC_{50} = 5.8 μM) as well as to a piperidin-1-ylmethyl group in **25** (IC_{50} = 4.6 μM) resulted in reduced activities, as compared to compounds **12** and **11**. Compound **26** with a polar -CH₂NH₂ group at the 5-position (of the thiophene core) is still a strong inhibitor with an IC_{50} of 2.0 μM , although it exhibited ~ 3 -fold activity reduction as compared to **12**. However, moving the -CH₂NH₂ group to the 4-position in compound **27** suffered a major activity loss. Compound **28** with the amine group at both positions is inactive. Similarly, compound **29** with two -CH₂OH groups is also a weak inhibitor. Activities for compounds **26-29** suggest polar groups are not favorable at 4- or 5-position. In addition, very low activity for compound **30** suggests a smaller aromatic ring at 4- and 5-positions is disfavored. Lack of inhibition for compounds **31** and **32** with *meta*-substitutions at the 4- and 5-positions indicated that *para*-substitution (e.g., those in compound **10**) is more favorable for p300 HAT inhibition. Compound **33** (Chart 1) was synthesized with a -Br substituent at the 3-position of the thiophene core. It turned out to be still a strong inhibitor with an IC_{50} of 1.8 μM , while 3-Br reduces the inhibitory activity by ~ 3 -fold (as compared to **12**).

Finally, compounds **34-40** (Chart 1) were synthesized to study SARs for the central core. Furan analogs **34** and **35** with IC_{50} values of 4.9 and 3.0 μM , respectively, were found to be significantly less active than thiophene compounds **12** and **11**, suggesting a furan core is less favored. While the thiazole compound **36** (IC_{50} = 2.4 μM) exhibited an improved activity as compare to its thiophene analog **1**, the thiazole compound **37** (IC_{50} = 8.6 μM) is more than $13\times$ less active than its thiophene analog **12**. Loss of activity for compounds **38** and **39** shows that the 5-substituent is of importance to the inhibition of p300 HAT. Moreover, compound **40** with a 6-membered pyrazine core was found to be significantly less active

than its thiophene analog **11**. These results suggest thiophene is the most favorable aromatic core structure for this series of inhibitors.

Compound **12** is competitive against histone.

We next performed steady-state enzyme kinetics studies to investigate the mode of inhibition for the most potent inhibitor **12**. Inhibitory activities of compound **12** were determined with varying concentrations of the cofactor Ac-CoA and the substrate histone. As shown in Figure 2A (left), IC₅₀ values of **12** did not change with increasing concentrations of Ac-CoA (from 0.5 - 8 μM, or 0.07-1.2× K_m ²⁵), indicating compound **12** is likely a non-competitive inhibitor against the enzyme cofactor. Its inhibitory activities were found to be reduced in a linear manner (Figure 2A) when increasing concentrations of the substrate histone peptide (2 - 100 μM) were used in the assay, suggesting compound **12** is a competitive inhibitor against the substrate histone.

Next, we used a reported Alpha (amplified luminescent proximity homogeneous assay) assay¹⁶ to confirm this finding. Upon excitation by a laser beam (680 nm), histone H4(1–21) peptide coated donor beads generate singlet oxygen radicals, which can travel for a very short distance (<200 nm) in the solution and cannot reach the free acceptor beads. The binding between the histone peptide and p300 HAT brings the donor and acceptor beads together, which allows the radicals to activate the p300 HAT coated acceptor beads and produce luminescence at 570 nm. Use of histone H4 is because the assay with histone H3 did not produce a luminescence signal, presumably due to a weaker binding between p300 HAT and histone H3. As shown in Figure 2B, compound **12** can disrupt the binding between the protein and histone H4, and reduce the Alpha-signal in a dose-dependent manner (IC₅₀ = 13.5 μM). This is in contrast to Ac-CoA-competitive inhibitor A-485¹⁶, which did not affect the binding between p300 HAT and histone H4. In addition, such binding was not interfered by inactive compound **28** (Fig. 2B). Increasing concentrations of compound **12** did not significantly affect the Alpha-signals using a biotinylated His6 peptide that can directly link the donor and acceptor beads (Figure S2), showing **12** does not interfere with the singlet oxygen radicals or His6 tag. Taken together, these results indicate the inhibitor **12** is competitive against the substrate histone, which are of interest in that due to a different mode of inhibition, histone-competitive inhibitor **12** might have a different cellular activity or selectivity, as compared to Ac-CoA-competitive inhibitors A-485 and C646^{16, 20}.

Docking studies.

We next performed molecular modeling to find possible binding structures of the most potent inhibitor **12** in p300 HAT. The program Glide in Schrödinger small-molecule drug discovery software suite was used for the docking studies, with the crystal structure of human p300 HAT in complex with Ac-CoA (PDB code 4PZS)²⁶ as a template.

Since compound **12** is a competitive inhibitor against the substrate histone, Ac-CoA was treated as an integrate part of the protein. Upon protein structure preparation as well as docking grid generation, compound **12** was docked into the protein-Ac-CoA complex and the results are shown in Figure 3. The inhibitor can be favorably docked into the protein, as the 10 distinct docking conformations of compound **12** with the lowest energies exhibit

similar binding features (Figure 3A). One of the *tert*-butyl group of these conformations is predicted to insert into and have favorable hydrophobic interactions with the so-called “lysine channel”, through which the histone lysine sidechain inserts into p300 HAT, attacks the carbonyl of Ac-CoA, and gets acetylated. Residues Trp1436, Cys1438, Tyr1446 and Ser1396 form the lysine channel of p300 HAT (Figure 3B). As shown in Figure 3B, the *tert*-butyl group is predicted to be ~3.5 Å from these residues with favorable van de Waals interactions. The central thiophene core and the two *para-tert*-butylphenyl groups of these structures have extensive hydrophobic interactions with either upper or lower surface of the protein (Figure 3A/B). In addition, the positively charged, two amino groups of many of these docking structures form hydrogen bonds and have favorable electrostatic interactions with Asp1628 and Glu1505, as exemplified in Figure 3B. These favorable binding features are consistent with the strong inhibitory activity of compound **12**.

Moreover, the docking results might be used to rationalize some of the observed SARs. For example, H-bond/electrostatic interactions between -NH- (positively charged at physiological pH) and Asp1628 are predicted to contribute significantly to the binding of compound **12**. This could explain the loss of activity for compound **13** with an -O- linkage, which does not favorably interact with the (negatively charged) Asp1628 sidechain. Since an amide -CONH- mimics the positively charged -NH- in **12**, many of the amide compounds (e.g., compounds **2** and **6** in Table 1) are potent inhibitors. Docking results also suggest favorable interactions of **12** with the lysine channel are important for tight binding. This could explain weak or no activities for compounds **30-32**, which do not have a *para*-substituent or have a *meta*-substituent which might not favorably interact with the lysine channel residues of the protein.

Enzyme selectivity.

Humans have three classes of histone/protein lysine acetyltransferases with distinct conserved motifs and structures, including p300/CBP, Gcn5-related N-acetyltransferase (GNAT) and MYST (MOZ, Ybf2, Sas2 and Tip60) family of HATs. Compound **12** was tested for its activities against selected HATs from these three classes of HATs. CBP is a homolog of p300. The HAT domains of CBP and p300 exhibit 87% identity in sequence. PCAF (p300/CBP associating factor) is a member of the GNAT family, while Myst3 belongs to the MYST family of HATs. P300/CBP HATs have a distinct sequence and 3-dimensional structure from the GNAT and MYST HAT proteins. As shown in Table 2, compound **12** was found to be also a strong inhibitor of human CBP HAT with an IC₅₀ of 1.2 μM, comparable to its IC₅₀ against p300 HAT. However, compound **12** did not significantly inhibit the activity of PCAF and Myst3 even at 50 μM, showing a high selectivity for p300/CBP HAT. In addition, since the initial hit compound **1** was for SAR studies targeting LSD1, both compounds **1** and **12** did not significantly inhibit activity of LSD1 at 50 μM.

Inhibition of cellular histone acetylation.

Ability of compound **12** to inhibit cellular p300/CBP HAT was evaluated. Also included in the experiment are an inactive compound **28** and a known inhibitor A-485. Kasumi-1 leukemia cells were treated with increasing concentrations of these compounds for 12h. Histone was extracted and subjected to electrophoresis separation and Western blot staining

to determine levels of acetylation at various lysine residues. As shown in Figure 4, compound **12** was found to significantly inhibit cellular acetylation of histone H3K9, H3K18 and H3K27 at 5 and 10 μM , in a dose dependent manner. H3K27 seems to be the most sensitive cellular substrate of p300 HAT. Inactive compound **28** was found to have no significant activity against acetylation of these histone residues. As compared to A-485 (enzyme IC_{50} of 60 nM ¹⁶), compound **12** is less active against acetylation of H3K27 and K18, which is consistent with the enzyme activities of these compounds. However, compound **12** seems to exhibit more potent cellular activity against acetylation of H3K9. These differences might be due to different mode of inhibition (competitive against histone vs. Ac-CoA) or cell permeability for the two compounds.

Inhibition of tumor cell proliferation.

Activity of compound **12** was tested against proliferation of several tumor cell lines in which p300/CBP HAT is of importance. First, ER-mediated transcription is critical to ER+ breast cancer. It is an ordered, stepwise assembly of ER and coactivator proteins for gene expression^{10, 27}. Upon binding with an estrogen molecule in cytoplasm, ER undergoes conformational changes, forms a homodimer, and is translocated into the nucleus, where ER binds to estrogen response element, a short segment of DNA within a gene promoter. Next, a steroid receptor coactivator (SRC) protein binds to ER, followed by recruitment of p300 through its SRC-binding SID domain⁹. P300 HAT activity is required for the ER-mediated gene expression, because a mutant p300 without the enzyme function failed to activate it¹⁰. Given the critical role of p300-mediated histone acetylation in the ER signaling pathway, compound **12** was assessed for its activity against the ER+ breast cancer cell line MCF-7. In addition, ER antagonist tamoxifen is widely used in the clinic to treat ER+ breast cancer by suppressing ER mediated gene transcription. However, many patients eventually develop resistance to tamoxifen and die of the cancer. In our previous work^{28, 29}, we have developed MCF-7 derivative cells that were made resistant to tamoxifen. Activity of compound **12** was also tested against tamoxifen-resistant MCF-7 to find whether inhibition of HAT can affect growth of these cells. As summarized in Table 3, compound **12** exhibited strong antiproliferative activity against parent MCF-7 cells ($\text{EC}_{50} = 2.8 \mu\text{M}$) as well as tamoxifen-resistant cells ($\text{EC}_{50} = 3.4 \mu\text{M}$). These results show that inhibition of p300-mediated histone acetylation can inhibit growth of MCF-7 breast cancer cells and such activity is independent upon the status of tamoxifen resistance, suggesting the p300 HAT inhibitor could have potential clinical applications in breast cancer therapy.

Moreover, p300 HAT activity has been reported to play important roles in pancreatic cancer³⁰ and acute myeloid leukemia caused by oncogene RUNX1-ETO³¹. Activity of compound **12** was evaluated against two pancreatic cancer cells PANC-1 and MDA-PANC-28 and RUNX1-ETO leukemia cell line Kasumi-1. As shown in Table 3, compound **12** showed potent activities against proliferation of the two pancreatic cancer cells with EC_{50} values of 1.0 and 2.8 μM . It also inhibited growth of Kasumi-1 cells with an EC_{50} of 2.6 μM .

Inactive compounds **28** and **31** exhibited no inhibitory activities against proliferation of these cancer cells, supporting activity of compound **12** is related to inhibition of p300 HAT. Surprisingly, although A-485 exhibited more potent activity ($\text{EC}_{50} = 0.33 \mu\text{M}$) against

Kasumi-1 leukemia cells, it had no significant activity against proliferation of breast and pancreatic cancer cells (Table 3). These differences might be due to different modes of inhibition (competitive against histone vs. Ac-CoA) or cell permeability for compound **12** and A-485.

Gene expression profiling.

RNA sequencing was used to investigate how treatment with p300 HAT inhibitor **12** affects gene expression in ER+ breast cancer MCF-7 cells. Upon starvation (i.e., culturing in charcoal treated FBS without hydrophobic hormones including estrogens) for 7 days, MCF-7 cells were supplemented with estradiol (10 nM), followed by treatment with compound **12** for 2 days. Total RNA from three groups of MCF-7 cells, including starved, control (with estradiol) and treated (with estradiol and compound **12**) groups, was purified, prepared and sequenced. RNA sequencing data were mapped onto the human genome and gene expression profiles were determined and normalized. Genes with significantly changed expression levels were determined using a two-sided parametric *t*-test with the *p* value of <0.05. Gene set enrichment analysis (GSEA)³² was used to analyze significant gene expression changes between these three groups of MCF-7 cells.

First, to determine whether the observed cellular activities of compound **12** are due to inhibition of p300 HAT, we used GSEA to compare the transcriptional profile of the **12**-treated MCF-7 cells with a publicly available p300 transcriptional signature (GSE31873), which was derived from siRNA-mediated p300 knockdown in C4-2B prostate cancer cells³³. As shown in Figure 5A, there is a strong concordance between the two transcriptional signatures: Genes suppressed by compound **12** were strongly enriched among those suppressed by p300 knockdown, with normalized enrichment score (NES) of -3.32 and *p* value of <0.001. This result demonstrates that treatment with the p300 HAT inhibitor mimics the transcriptional footprint of p300 depletion and supports that p300 HAT is the cellular target of compound **12**.

Next, activity of compound **12** in the ER signaling pathway was analyzed. As compared to starved cells, supplementation with estradiol potentially caused upregulation as well as downregulation of several publicly available ER-related gene signatures in the control group of MCF-7 cells (Figure S3). Importantly, treatment with compound **12** counteracted such estrogen-induced gene transcription: The gene set upregulated by estradiol was strongly downregulated upon treatment with **12** (Figure 5B, NES = -9.19 and *p* < 0.001), and the genes suppressed by estradiol were significantly upregulated by compound **12** (Figure 5C, NES = 7.41 and *p* < 0.001). These results are consistent with previous studies showing p300 HAT is essential for ER-mediated gene expression, and demonstrate that pharmacological inhibition of p300 HAT can offset the effects of estrogen in gene regulation.

Moreover, we investigated gene expression changes caused by compound **12** in the context of cancer biology and therapy. As shown in Figure 5D, global gene expression profiling analysis revealed that inhibition of p300 HAT by compound **12** counteracted estradiol and caused significant suppression of a number of estrogen-induced, cancer-related gene sets, including E2F and c-Myc gene signatures as well as those involved in cell proliferation, cell

cycle, mitosis, DNA replication, DNA repair and self-renewal (stemness) (Figure S4). Specifically for breast cancer, treatment with compound **12** downregulated a number of gene signatures that have previously been shown to be upregulated in multiple breast cancer patient datasets (as compared to normal breast tissues), associated with poor prognosis, cancer progression, invasion and relapse (Figure 5E). Collectively, these GSEA results show the importance of p300 HAT in breast and other types of cancer, as well as the perspective for pharmacological inhibition of p300 HAT (by e.g., compound **12**) in breast cancer therapy.

CONCLUSION

Histone acetylation by the HAT domain of p300/CBP has been found to play critical roles in many nuclear receptor-regulated signaling pathways, such as ER, AR and peroxisome proliferator-activated receptors (PPAR)³⁴. Dysfunction of these gene transcription programs has been found in a number of diseases such as cancer and obesity. Moreover, p300/CBP has been found to directly contribute to oncogenesis (e.g., in RUNX1-ETO leukemia) or be part of a fusion oncogene due to chromosome translocation^{7, 14, 15}. Therefore, drug-like inhibitors of p300/CBP HAT are needed, which could be useful chemical probes and potential therapeutics for these indications. In addition, p300 and CBP are large proteins (~2,400 amino acids) with multiple other domains playing important physiological roles. They also share a high degree of homology with many duplicate functions. Given these two points, cell-permeable, small-molecule inhibitors of the HAT domain of p300/CBP are particularly useful for studying biological functions of p300/CBP HAT, because observed activities by genetic knockdown/knockout of p300 or CBP might not be relevant.

Compound screening followed by medicinal chemistry studies have led to the discovery of tri-substituted thiophene compound **12** that is a novel inhibitor with an IC₅₀ of 620 nM against p300 HAT and 1.2 μM against CBP HAT. It did not significantly inhibit two other major human HATs PCAF and Myst3 at 50 μM, showing a high selectivity. Biochemical studies showed that compound **12** is competitive against the substrate histone and non-competitive against the cofactor Ac-CoA, showing a distinct mode of inhibition from previous studied inhibitors C646 and A-485. Docking studies of **12** into the histone binding pocket of the p300 HAT structure provided possible binding models of the inhibitor in the protein. In addition, compound **12** was found to be cell-permeable and inhibit cellular acetylation at several histone lysine residues, with H3K27 being the most sensitive substrate. With EC₅₀ of ~3 μM, compound **12** strongly inhibited proliferation of ER⁺ breast cancer cell line MCF-7, regardless of its sensitivity or resistance to the commonly used estrogen antagonist tamoxifen, suggesting the potential therapeutic application of this compound in the context of endocrine resistance. Compound **12** also exhibited strong activity against growth of several pancreatic cancer cells and RUNX1-ETO leukemia cell Kasumi-1, in which p300 HAT is known to be important^{30, 31}.

Global gene transcription profiling was performed to investigate the cellular target of compound **12** as well as the mechanism for its observed biological activities in MCF-7 cells. First, the overall transcriptional changes upon treatment with compound **12** recapitulated those caused by siRNA-mediated p300 knockdown. This result, together with its inhibitory

activity in cellular histone lysine acetylation, support that p300 HAT is the cellular target of compound **12**. Second, inhibition of p300 HAT activity by compound **12** significantly offset estrogen-induced gene expression, showing p300 HAT is essential for the ER activity. Moreover, treatment with compound **12** strongly downregulated a number of (general) cancer-related gene signatures, as well as gene sets that have been identified in the clinic for the progression, invasion, relapse and poor prognosis of breast cancer. These results, together with the compound's potent antiproliferative activities against several types of cancer cells, suggest that pharmacological inhibition of p300 HAT is a useful therapeutic approach to cancer treatment.

In conclusion, our results demonstrate that compound **12** is not only a useful small-molecule probe for biological studies of p300/CBP HAT, but also a novel pharmacological lead for further drug development targeting breast and other types of cancer.

Experimental Section

All chemicals for synthesis were purchased from Alfa Aesar (Ward Hill, MA) or Aldrich (Milwaukee, WI). The identity of the synthesized compounds was characterized by ^1H and ^{13}C NMR on a Varian (Palo Alto, CA) 400-MR spectrometer and mass spectrometer (Shimadzu LCMS-2020). The identity of the potent inhibitors was confirmed with high resolution mass spectra (HRMS) using an Agilent 6550 iFunnel quadrupole-time-of-flight (Q-TOF) mass spectrometer with electrospray ionization (ESI). The purities of the final compounds were determined to be >95% with a Shimadzu Prominence HPLC using a Zorbax C18 (or C8) column (4.6 × 250 mm) monitored by UV at 254 nm.

General method A (reactions i-iv).

To a mixture of 4,5-Dibromothiophene-2-carboxylic acid **41** (2.86 g, 10 mmol), 1-ethyl-3-(3-dimethylaminopropyl)-carbodiimide (1.71 g, 11 mmol), 1-hydroxybenzotriazole (1.48 g, 11 mmol) in dichloromethane (20 mL), 1-BOC-4-(aminomethyl)piperidine (2.57 g, 12 mmol) and triethylamine (2.8 mL, 20 mmol) in CH_2Cl_2 (10 mL) were added slowly at 0 °C. The reaction mixture was stirred at room temperature for 1 h and quenched by adding saturated NaHCO_3 (50 mL). The product was extracted with dichloromethane (3 × 50 mL) and the combined organic layers were washed with water and brine, dried over Na_2SO_4 . Upon removal of the solvent, the product was purified by column chromatography (silica gel, *n*-hexanes: ethyl acetate from 10:1 to 2:1) to give the amide **42** as a white solid (4.63 g, 96% yield).

A mixture of **42** (0.4 mmol), Ar^1 -boronic acid or its pinacol ester (0.42 mmol), tetrakis(triphenylphosphine)palladium (13.9 mg) and sodium carbonate (84.8 mg, 0.8 mmol) in 1,4-dioxane/ H_2O (6 mL, 5:1) were heated to 80 °C for 12 h. The reaction was then quenched with brine (10 mL). The product was extracted with diethyl ether (3 × 20 mL) and the combined organic layers were washed with water and brine, dried over Na_2SO_4 . Upon removal of the solvent, the product was purified by column chromatography (silica gel, *n*-hexanes: ethyl acetate from 5:1 to 1:2) to give 5- Ar^1 substituted thiophene product as a white solid (60-90% yield). The product thus obtained (0.2 mmol) was added into a solution of Ar^2 -boronic acid or its pinacol ester (0.21 mmol), tetrakis(triphenylphosphine)palladium (7

mg) and sodium carbonate (42.4 mg, 0.4 mmol) in 1,4-dioxane/H₂O (5/1 mL). The mixture was heated to 100 °C for 12 h. Similar workup and purification gave 4,5-di-substituted thiophene compound **43** as a white solid (60-90% yield).

To a solution of **43** (0.1 mmol) in dichloromethane (2 mL) at 0 °C, HCl (0.1-0.2 mL, 4 N in 1,4-dioxane) was added slowly and then stirred at room temperature for 12 h. Upon removal of the solvent carefully, the residual oil was treated with anhydrous diethyl ether and vacuum dried to give the target compound (white powder) as a hydrochloric salt (90-100% yield).

General method B (reactions v-vii).

To a solution of 4,5-dibromothiophene-2-carboxaldehyde **44** (5.40 g, 20 mmol) in MeOH (40 mL), NaBH₄ (0.79 g, 21 mmol) was added slowly 0 °C. The reaction mixture was stirred at room temperature for 1 h and quenched with water (50 mL). The product was extracted with diethyl ether (3 × 100 mL) and the combined organic layers were washed with water and brine, dried over Na₂SO₄. Upon removal of the solvent carefully, the residual oil was dried and used in the next step without purification. It was dissolved in DMF (20 mL) and the solution was cooled to 0 °C. Cyanuric chloride (3.69 g, 20 mmol) was added slowly at 0 °C and stirred at room temperature for 10 h. The reaction was quenched with saturated NaHCO₃ (50 mL). The product was extracted with diethyl ether (3 × 100 mL) and the combined organic layers were washed with water and brine, dried over Na₂SO₄. Removal of the solvents *in vacuo* afforded compound **45** as a colorless oil, which is used without purification. To a solution of an amine (10 mmol) and potassium carbonate (1.38 g, 10 mmol) in DMF (10 mL), **45** (1.45 g, 5 mmol) in DMF (10 mL) was added slowly at 0 °C and the mixture was stirred at room temperature for 10 h. Upon quenching with saturated NaHCO₃ (50 mL), the product was extracted with diethyl ether (3 × 50 mL) and the combined organic layers were washed with water and brine, dried over Na₂SO₄. A column chromatography (silica gel, hexanes: ethyl acetate from 40:1 to 2:1) for the residue oil gave compound **46** as a pale-yellow oil (60-85% yield for the three steps).

Suzuki coupling reactions of compound **46** as well as deprotection of the BOC group were performed as described above, to produce the target compounds.

General method C (reactions viii and ix).

4-Bromothiazole-2-carbaldehyde **48** (1.92 g, 10 mmol) and N-bromosuccinimide (NBS, 1.78 g, 10 mmol) were dissolved in dichloromethane (20 mL) and stirred at room temperature for 12 h. Upon removal of the solvent carefully, the residue was purified by column chromatography (silica gel, hexanes: ethyl acetate from 40:1 to 10:1) to give 4,5-dibromothiazole-2-carbaldehyde **49** as a white solid (433 mg, 16% yield). Conversion of aldehydes **48** and **49** to compounds **38** and **37** followed the reactions described above.

4,5-Dibromothiazole-2-carbaldehyde **49** (406 mg, 1.5 mmol) or **48**, sodium chlorite (190 mg, 2.1 mmol) and 2-methylbut-2-ene (1.6 mL, 15 mmol) were dissolved by ^tBuOH/H₂O (5/1 mL). Sodium dihydrogen phosphate (900 mg in 5 mL H₂O) was added slowly into the reaction mixture. The mixture was stirred at rt for 12 h. The reaction was then quenched with brine (10 mL). The product was extracted with diethyl ether (3 × 10 mL) and the

combined organic layers were washed with water and brine, dried over Na_2SO_4 . The volatiles were removed *in vacuo* to afford acid **51** as a crude oil, which was used directly in the next step without further purification.

4,5-bis(4-(*tert*-Butyl)phenyl)-*N*-(piperidin-4-ylmethyl)thiophene-2-carboxamide hydrochloride (1) was prepared from 4,5-dibromothiophene-2-carboxylic acid, following the general method A, as a hydrochloric acid salt (white powder). ^1H NMR (400 MHz, DMSO-d_6): δ 8.69 (br, 3H), 7.92 (s, 1H), 7.38-7.35 (m, 4H), 7.26-7.21 (m, 4H), 3.26-3.23 (m, 2H), 3.17 (br, 2H), 2.85-2.79 (m, 2H), 1.82-1.79 (m, 3H), 1.42-1.36 (m, 2H), and 1.27 (s, 18H); ^{13}C NMR (100 MHz, DMSO-d_6): 161.1, 150.8, 149.8, 141.5, 137.6 (2), 132.7, 131.4, 130.4, 128.4, 128.2, 125.6, 125.3, 43.8, 42.8, 34.4, 34.3, 33.7, 31.1, 31.0, and 26.22; MS (ESI) calcd for $(\text{C}_{31}\text{H}_{41}\text{N}_2\text{OS})^+ [\text{M}+\text{H}]^+$ 489.7, found 489.6.

4,5-bis(4-(Furan-3-yl)phenyl)-*N*-(piperidin-4-ylmethyl)thiophene-2-carboxamide hydrochloride (2) was prepared from 4,5-dibromothiophene-2-carboxylic acid, following the general method A, as a hydrochloric acid salt (white powder). ^1H NMR (400 MHz, DMSO-d_6): δ 8.89 (br, 1H), 8.76 (br, 1H), 8.58 (br, 1H), 8.21 (s, 2H), 8.00 (s, 1H), 7.74 (s, 2H), 7.61-7.59 (m, 4H), 7.31-7.28 (m, 4H), 6.97 (s, 2H), 3.27-3.23 (m, 2H), 3.19 (br, 2H), 2.86-2.78 (m, 2H), 1.85-1.82 (m, 3H), and 1.42-1.36 (m, 2H); ^{13}C NMR (100 MHz, DMSO-d_6): 161.0, 147.1, 144.5, 141.6, 139.9, 139.6, 138.6, 138.0, 137.8, 133.9, 132.08, 131.96, 131.65, 131.54, 131.0, 130.8, 129.2, 129.0, 125.9, 125.7, 108.6, 43.8, 42.8, 33.8, and 26.2; MS (ESI) calcd for $(\text{C}_{31}\text{H}_{29}\text{N}_2\text{O}_3\text{S})^+ [\text{M}+\text{H}]^+$ 509.6, found 509.5.

4,5-bis(4'-Methoxy-[1,1'-biphenyl]-4-yl)-*N*-(piperidin-4-ylmethyl)thiophene-2-carboxamide hydrochloride (3) was prepared from 4,5-dibromothiophene-2-carboxylic acid, following the general method A, as a hydrochloric acid salt (white powder). ^1H NMR (400 MHz, DMSO-d_6): δ 8.91 (br, 1H), 8.79 (br, 1H), 8.62 (br, 1H), 8.02 (s, 1H), 7.70-7.56 (m, 8H), 7.38-7.35 (m, 4H), 7.02-6.99 (m, 4H), 3.78 (s, 6H), 3.27-3.23 (m, 2H), 3.19 (br, 2H), 2.87-2.79 (m, 2H), 1.85-1.82 (m, 3H), and 1.42-1.36 (m, 2H); ^{13}C NMR (100 MHz, DMSO-d_6): 161.1, 159.2, 159.0, 141.6, 139.6, 138.6, 138.1, 137.7, 133.8, 131.64, 131.57, 131.46, 131.38, 129.3, 129.2, 127.72, 127.66, 126.5, 126.2, 114.5, 114.4, 55.2, 43.8, 42.9, 33.8, 28.1, and 26.3; MS (ESI) calcd for $(\text{C}_{37}\text{H}_{37}\text{N}_2\text{O}_3\text{S})^+ [\text{M}+\text{H}]^+$ 589.8, found 589.9.

5-(4-(*tert*-Butyl)phenyl)-4-(4-(furan-3-yl)phenyl)-*N*-(piperidin-4-ylmethyl)thiophene-2-carboxamide hydrochloride (4) was prepared from 4,5-dibromothiophene-2-carboxylic acid, following the general method A, as a hydrochloric acid salt (white powder). ^1H NMR (400 MHz, DMSO-d_6): δ 8.90 (br, 1H), 8.76 (br, 1H), 8.61 (br, 1H), 8.21 (s, 1H), 7.97 (s, 1H), 7.92 (s, 1H), 7.74 (s, 1H), 7.59 (s, 1H), 7.36-7.23 (m, 6H), 6.97 (s, 2H), 3.27-3.23 (m, 2H), 3.18 (br, 2H), 2.85-2.79 (m, 2H), 1.83-1.80 (m, 3H), 1.40-1.36 (m, 2H), and 1.26 (s, 9H); ^{13}C NMR (100 MHz, DMSO-d_6): 161.1, 151.0, 144.4, 142.0, 139.6, 137.8, 137.5, 134.1, 131.0, 129.0, 128.44, 128.40, 128.3, 125.74, 125.70, 125.4, 108.6, 43.8, 42.9, 34.4, 33.8, 31.1, and 26.3; MS (ESI) calcd for $(\text{C}_{31}\text{H}_{35}\text{N}_2\text{O}_2\text{S})^+ [\text{M}+\text{H}]^+$ 499.7, found 499.5.

4-(4-(Aminomethyl)phenyl)-5-(4-(*tert*-butyl)phenyl)-*N*-(piperidin-4-ylmethyl)thiophene-2-carboxamide hydrochloride (5) was prepared from 4,5-dibromothiophene-2-carboxylic acid, following the general method A, as a hydrochloric acid

salt (white powder). ^1H NMR (400 MHz, D_2O): δ 7.76 (s, 1H), 7.25 (d, $J = 7.6$ Hz, 2H), 7.14 (d, $J = 7.6$ Hz, 2H), 6.97 (d, $J = 7.3$ Hz, 2H), 6.90 (d, $J = 7.3$ Hz, 2H), 4.03 (s, 2H), 3.45 (d, $J = 11.7$ Hz, 2H), 3.29-3.27 (m, 2H), 2.95 (t, $J = 12.6$ Hz, 2H), 1.98-1.94 (m, 3H), 1.52-1.42 (m, 2H), and 0.97 (s, 9H); ^{13}C NMR (100 MHz, D_2O): 163.4, 151.3, 143.8, 137.3, 136.1, 134.3, 131.6, 129.9, 129.4, 129.1, 128.5, 128.1, 125.4, 44.3, 43.6, 42.6, 33.9, 33.5, 30.5, and 26.1; MS (ESI) calcd for $(\text{C}_{28}\text{H}_{36}\text{N}_3\text{OS})^+ [\text{M}+\text{H}]^+$ 462.7, found 462.6.

5-(4-(Furan-3-yl)phenyl)-4-(4-(piperidin-1-ylmethyl)phenyl)-N-(piperidin-4-ylmethyl)thiophene-2-carboxamide hydrochloride (6) was prepared from 4,5-dibromothiophene-2-carboxylic acid, following the general method A, as a hydrochloric acid salt (white powder). ^1H NMR (400 MHz, DMSO-d_6): δ 10.54 (br, 1H), 8.94 (br, 1H), 8.84 (br, 1H), 8.64 (br, 1H), 8.22 (s, 1H), 8.03 (s, 1H), 7.75 (s, 1H), 7.60 (d, $J = 7.8$ Hz, 4H), 7.36 (d, $J = 7.8$ Hz, 2H), 7.28 (d, $J = 7.8$ Hz, 2H), 6.97 (s, 1H), 4.24 (s, 4H), 3.25-3.24 (m, 4H), 3.19-3.16 (m, 2H), 2.86-2.78 (m, 4H), 1.83-1.78 (m, 6H), 1.70-1.66 (m, 1H), and 1.48-1.34 (m, 2H); ^{13}C NMR (100 MHz, DMSO-d_6): 161.0, 144.6, 142.2, 140.0, 138.2, 137.3, 136.6, 132.1, 131.8, 131.6, 131.5, 129.3, 129.0, 126.0, 125.2, 115.5, 108.6, 58.6, 51.7, 43.9, 42.9, 33.7, 26.3, 22.2, and 21.5; MS (ESI) calcd for $(\text{C}_{33}\text{H}_{38}\text{N}_3\text{O}_2\text{S})^+ [\text{M}+\text{H}]^+$ 540.7, found 540.6.

5-(4-(tert-Butyl)phenyl)-4-(4-(piperazin-1-ylmethyl)phenyl)-N-(piperidin-4-ylmethyl)thiophene-2-carboxamide hydrochloride (7) was prepared from 4,5-dibromothiophene-2-carboxylic acid, following the general method A, as a hydrochloric acid salt (white powder). ^1H NMR (400 MHz, CD_3OD): δ 7.83 (s, 1H), 7.58 (d, $J = 8.1$ Hz, 2H), 7.42 (d, $J = 8.1$ Hz, 2H), 7.37 (d, $J = 8.4$ Hz, 2H), 7.23 (d, $J = 8.4$ Hz, 2H), 4.44 (s, 2H), 3.61 (br, 4H), 3.56 (br, 4H), 3.43 (d, $J = 8.1$ Hz, 2H), 3.35 (d, $J = 6.0$ Hz, 2H), 3.00 (t, $J = 12.2$ Hz, 2H), 2.03-1.98 (m, 3H), 1.55-1.45 (m, 2H), and 1.31 (s, 9H); ^{13}C NMR (100 MHz, CD_3OD): 164.3, 153.1, 145.8, 139.2, 138.5, 138.1, 134.2, 132.8, 132.3, 131.6, 130.9, 130.0, 126.9, 61.4, 58.7, 45.4, 45.0, 42.2, 35.6, 31.6, 28.5, and 27.8; MS (ESI) calcd for $(\text{C}_{32}\text{H}_{43}\text{N}_4\text{OS})^+ [\text{M}+\text{H}]^+$ 531.8, found 531.7.

5-(4-(tert-Butyl)phenyl)-4-(furan-3-yl)-N-(piperidin-4-ylmethyl)thiophene-2-carboxamide hydrochloride (8) was prepared from 4,5-dibromothiophene-2-carboxylic acid, following the general method A, as a hydrochloric acid salt (white powder). ^1H NMR (400 MHz, DMSO-d_6): δ 8.90 (br, 1H), 8.73 (br, 1H), 8.59 (br, 1H), 7.97 (s, 1H), 7.65 (s, 1H), 7.44-7.34 (m, 5H), 6.29 (s, 1H), 3.27-3.24 (m, 2H), 3.17 (br, 2H), 2.84-2.80 (m, 2H), 1.83-1.78 (m, 3H), 1.40-1.37 (m, 2H), and 1.29 (s, 9H); ^{13}C NMR (100 MHz, DMSO-d_6): 161.4, 151.7, 144.1, 140.4, 138.2, 130.7, 130.5, 129.2, 129.1, 126.3, 126.0, 120.8, 110.6, 44.2, 43.2, 34.9, 34.1, 31.4, and 26.6; MS (ESI) calcd for $(\text{C}_{25}\text{H}_{31}\text{N}_2\text{O}_2\text{S})^+ [\text{M}+\text{H}]^+$ 423.6, found 423.5.

5-(4-(tert-Butyl)phenyl)-N-(piperidin-4-ylmethyl)-4-(pyridin-3-yl)thiophene-2-carboxamide hydrochloride (9) was prepared from 4,5-dibromothiophene-2-carboxylic acid, following the general method A, as a hydrochloric acid salt (white powder). ^1H NMR (400 MHz, DMSO-d_6): δ 9.00 (br, 1H), 8.92 (br, 1H), 8.74 (br, 1H), 8.70 (br, 1H), 8.17 (br, 2H), 7.85 (s, 1H), 7.61-7.55 (m, 2H), 7.40-7.26 (m, 4H), 3.27-3.18 (m, 4H), 2.83-2.80 (m, 2H), 1.84-1.79 (m, 3H), 1.42-1.39 (m, 2H), and 1.26 (s, 9H); ^{13}C NMR (100 MHz, DMSO-d_6): 161.2, 152.1, 145.2, 143.8, 143.3, 142.8, 139.2, 134.1, 132.2, 131.1, 129.5, 129.1,

126.6, 126.5, 44.3, 43.2, 34.9, 34.1, 31.4, and 26.6; MS (ESI) calcd for (C₂₆H₃₂N₃OS)⁺ [M+H]⁺ 434.6, found 434.4.

1-(4,5-bis(4'-Methoxy-[1,1'-biphenyl]-4-yl)thiophen-2-yl)-N-(piperidin-4-ylmethyl)methanamine hydrochloride (10) was prepared from 4,5-dibromothiophene-2-carboxaldehyde, following the general method B, as a hydrochloric acid salt (white powder). ¹H NMR (400 MHz, DMSO-d₆): δ 9.46 (br, 1H), 9.39 (br, 1H), 8.90 (br, 1H), 8.72 (br, 1H), 7.69 (s, 1H), 7.63-7.54 (m, 8H), 7.34 (d, *J* = 8.2 Hz, 4H), 7.01 (d, *J* = 8.2 Hz, 4H), 4.41 (s, 2H), 3.78 (s, 6H), 3.29-3.26 (m, 2H), 2.94 (br, 2H), 2.87-2.79 (m, 2H), 2.08 (br, 1H), 1.98-1.92 (m, 2H), and 1.49-1.39 (m, 2H); ¹³C NMR (100 MHz, DMSO-d₆): 159.2, 159.1, 139.4, 139.2, 138.6, 137.2, 134.2, 133.9, 131.7, 131.4, 129.4, 129.2, 127.76, 127.70, 126.9, 126.6, 126.4, 126.0, 114.54, 114.50, 55.3, 50.7, 44.7, 42.5, 30.60, 30.55, and 26.1; MS (ESI) calcd for (C₃₇H₃₉N₂O₂S)⁺ [M+H]⁺ 575.8, found 575.7.

1-(4,5-bis(4-(Furan-3-yl)phenyl)thiophen-2-yl)-N-(piperidin-4-ylmethyl)methanamine hydrochloride (11) was prepared from 4,5-dibromothiophene-2-carboxaldehyde, following the general method B, as a hydrochloric acid salt (yellow powder). ¹H NMR (400 MHz, DMSO-d₆): δ 9.54 (br, 2H), 9.03 (br, 1H), 8.88 (br, 1H), 7.46 (s, 1H), 7.16-7.12 (m, 8H), 4.35 (s, 2H), 3.26-3.23 (m, 2H), 2.92-2.88 (m, 2H), 2.84-2.79 (m, 2H), 2.54 (t, *J* = 7.4 Hz, 4H), 2.09 (br, 1H), 1.97-1.93 (m, 2H), 1.52 (p, *J* = 7.4 Hz, 4H), 1.46-1.39 (m, 2H), 1.32-1.23 (m, 4H), and 0.87 (t, *J* = 7.4 Hz, 6H); ¹³C NMR (100 MHz, DMSO-d₆): 144.5, 144.4, 139.8, 139.6, 139.1, 137.2, 134.04, 133.97, 131.79, 131.69, 131.62, 130.9, 129.2, 129.0, 126.0, 125.8, 125.3, 125.2, 108.58, 108.56, 50.6, 44.6, 42.4, 30.6, and 26.1; MS (ESI) calcd for (C₃₁H₃₁N₂O₂S)⁺ [M+H]⁺ 495.7, found 495.6.

1-(4,5-bis(4-(*tert*-Butyl)phenyl)thiophen-2-yl)-N-(piperidin-4-ylmethyl)methanamine hydrochloride (12) was prepared from 4,5-dibromothiophene-2-carboxaldehyde, following the general method B, as a hydrochloric acid salt (white powder). ¹H NMR (400 MHz, DMSO-d₆): δ 9.56 (br, 2H), 9.00 (br, 1H), 8.84 (br, 1H), 7.48 (s, 1H), 7.36 (d, *J* = 7.2 Hz, 4H), 7.20 (d, *J* = 7.2 Hz, 4H), 4.35 (s, 2H), 3.27-3.24 (m, 2H), 2.89 (br, 2H), 2.86-2.82 (m, 2H), 2.05 (br, 1H), 1.97-1.94 (m, 2H), 1.45-1.40 (m, 2H), and 1.27 (s, 18H); ¹³C NMR (100 MHz, DMSO-d₆): 150.5, 149.6, 139.0, 137.0, 134.3, 132.8, 131.4, 130.6, 128.4, 128.2, 125.7, 125.4, 50.6, 44.6, 42.3, 34.42, 34.34, 31.13, 31.05, 30.6, and 26.1; MS (ESI) calcd for (C₃₁H₄₃N₂S)⁺ [M+H]⁺ 475.8, found 475.7; HRMS (ESI⁺) calcd for C₃₁H₄₂N₂S [M+H]⁺ 475.3147, found 475.3145.

4-(((4,5-bis(4-(*tert*-Butyl)phenyl)thiophen-2-yl)methoxy)methyl)piperidine hydrochloride (13).

Starting from 4,5-dibromothiophene-2-carboxaldehyde, reactions v and vi gave 2-chloromethyl-4,5-dibromothiophene, which reacted with sodium salt of 1-BOC-4-hydroxymethylpiperidine, to give 4,5-dibromothiophen-2-ylmethyl 1-BOC-piperidin-4-ylmethyl ether. Reactions ii and iii (General method B) produced compound **13** as a hydrochloric acid salt (white powder). ¹H NMR (400 MHz, DMSO-d₆): δ 8.72 (br, 1H), 8.38 (br, 1H), 7.36 (d, *J* = 8.1 Hz, 2H), 7.33 (d, *J* = 8.1 Hz, 2H), 7.48 (s, 1H), 7.21 (d, *J* = 8.1 Hz, 2H), 7.17 (d, *J* = 8.1 Hz, 2H), 5.05 (s, 2H), 3.27-3.23 (m, 4H), 2.86-2.77 (m, 2H), 1.78-1.75 (m, 2H), 1.62 (br, 1H), and 1.26 (s, 18H); ¹³C NMR (100 MHz, DMSO-d₆):

150.4, 149.6, 138.8, 138.6, 136.7, 132.8, 131.7, 130.7, 128.4, 128.2, 125.6, 125.3, 65.0, 42.9, 40.8, 35.9, 34.4, 34.3, 31.10, 31.02, and 25.2; MS (ESI) calcd for (C₃₁H₄₂NOS)⁺ [M+H]⁺ 476.7, found 476.6.

***N*-((4,5-bis(4-*tert*-Butyl)phenyl)thiophen-2-yl)methyl)piperidin-4-amine hydrochloride (14)** was prepared from 4,5-dibromothiophene-2-carboxaldehyde, following the general method B, as a hydrochloric acid salt (white powder). ¹H NMR (400 MHz, DMSO-*d*⁶): δ 9.85 (br, 2H), 9.24 (br, 1H), 8.99 (br, 1H), 7.50 (s, 1H), 7.36 (d, *J* = 7.2 Hz, 4H), 7.20 (d, *J* = 7.2 Hz, 4H), 4.40 (s, 2H), 2.95 (br, 3H), 2.30 (br, 2H), 1.95 (m, 2H), and 1.27 (s, 18H); ¹³C NMR (100 MHz, DMSO-*d*⁶): 150.6, 149.7, 139.1, 137.1, 134.3, 132.8, 131.2, 130.6, 128.4, 128.2, 125.7, 125.4, 51.4, 41.4, 34.42, 34.34, 31.14, 31.06, 28.9, and 24.9; MS (ESI) calcd for (C₃₀H₄₁N₂S)⁺ [M+H]⁺ 461.7, found 461.6.

***N*-((4,5-bis(4-*tert*-Butyl)phenyl)thiophen-2-yl)methyl)-2-(piperidin-4-yl)ethanamine hydrochloride (15)** was prepared from 4,5-dibromothiophene-2-carboxaldehyde, following the general method B, as a hydrochloric acid salt (white powder). ¹H NMR (400 MHz, DMSO-*d*⁶): δ 9.55 (br, 2H), 8.99 (br, 1H), 8.81 (br, 1H), 7.47 (s, 1H), 7.35 (br, 4H), 7.20 (br, 4H), 4.35 (s, 2H), 3.23 (br, 2H), 2.98 (br, 2H), 2.80 (br, 2H), 1.78 (br, 1H), 1.65 (br, 2H), 1.35 (br, 2H), and 1.26 (s, 18H); ¹³C NMR (100 MHz, DMSO-*d*⁶): 150.5, 149.6, 138.9, 137.0, 134.1, 132.7, 131.4, 130.5, 128.4, 128.2, 125.7, 125.4, 44.0, 43.8, 43.0, 34.39, 34.31, 31.3, 31.1, 31.0, 30.6, and 28.0; MS (ESI) calcd for (C₃₂H₄₅N₂S)⁺ [M+H]⁺ 489.8, found 489.7.

***N*¹-((4,5-bis(4-*tert*-Butyl)phenyl)thiophen-2-yl)methyl)propane-1,3-diamine hydrochloride (16)** was prepared from 4,5-dibromothiophene-2-carboxaldehyde, following the general method B, as a hydrochloric acid salt (white powder). ¹H NMR (400 MHz, CDCl₃): δ 9.70 (br, 2H), 8.24 (br, 3H), 7.34 (s, 1H), 7.17-7.07 (m, 8H), 7.24 (d, *J* = 7.6 Hz, 4H), 4.22 (s, 2H), 3.29-3.20 (m, 2H), 2.47 (br, 2H), 1.34-1.32 (m, 2H), and 1.19 (s, 18H); ¹³C NMR (100 MHz, CDCl₃): 150.6, 149.8, 140.8, 137.7, 135.0, 132.9, 130.8, 129.0, 128.8, 128.7, 125.5, 125.4, 45.5, 44.0, 37.8, 34.62, 34.57, 31.44, 31.36, and 29.8; MS (ESI) calcd for (C₂₈H₃₉N₂S)⁺ [M+H]⁺ 435.7, found 435.6.

***N*¹-((4,5-bis(4-*tert*-Butyl)phenyl)thiophen-2-yl)methyl)hexane-1,6-diamine hydrochloride (17)** was prepared from 4,5-dibromothiophene-2-carboxaldehyde, following the general method B, as a hydrochloric acid salt (white powder). ¹H NMR (400 MHz, DMSO-*d*⁶): δ 9.34 (br, 2H), 7.87 (br, 3H), 7.44 (s, 1H), 7.38 (d, *J* = 8.2 Hz, 2H), 7.36 (d, *J* = 8.2 Hz, 2H), 7.21 (d, *J* = 8.2 Hz, 2H), 7.19 (d, *J* = 8.2 Hz, 2H), 4.35 (s, 2H), 2.94 (br, 2H), 2.76 (p, *J* = 7.4 Hz, 2H), 1.66 (p, *J* = 7.4 Hz, 2H), 1.54 (p, *J* = 7.4 Hz, 2H), 1.35-1.33 (m, 4H), and 1.27 (s, 18H); ¹³C NMR (100 MHz, DMSO-*d*⁶): 150.6, 149.7, 139.0, 137.0, 134.0, 132.7, 131.4, 130.5, 128.3, 128.2, 125.6, 125.4, 46.7, 46.1, 44.1, 34.4, 34.3, 31.1, 31.0, 26.7, 25.5, 25.3, and 25.2; MS (ESI) calcd for (C₃₁H₄₅N₂S)⁺ [M+H]⁺ 477.8, found 477.6.

1-((4,5-bis(4-*tert*-Butyl)phenyl)thiophen-2-yl)methyl)piperazine hydrochloride (18) was prepared from 4,5-dibromothiophene-2-carboxaldehyde, following the general method B, as a hydrochloric acid salt (white powder). ¹H NMR (400 MHz, DMSO-*d*⁶): δ 9.61 (br, 1H), 9.50 (br, 2H), 7.44 (s, 1H), 7.38-7.34 (m, 4H), 7.22-7.19 (m, 4H), 4.48 (s, 2H), 3.33 (s,

4H), 2.50 (s, 4H), and 1.27 (s, 18H); ^{13}C NMR (100 MHz, DMSO- d_6): 150.6, 149.7, 140.0, 138.6, 137.1, 132.6, 131.7, 130.4, 128.4, 128.3, 125.7, 125.4, 52.6, 47.1, 40.8, 34.4, 34.3, 31.1, and 31.0; MS (ESI) calcd for $(\text{C}_{29}\text{H}_{39}\text{N}_2\text{S})^+$ $[\text{M}+\text{H}]^+$ 447.7, found 447.6.

4-((4,5-bis(4-*tert*-Butyl)phenyl)thiophen-2-yl)methyl)morpholine hydrochloride (19) was prepared from 4,5-dibromothiophene-2-carboxaldehyde, following the general method B, as a hydrochloric acid salt (white powder). ^1H NMR (400 MHz, CDCl_3): δ 13.34 (br, 1H), 7.45 (s, 1H), 7.30 (d, $J = 7.6$ Hz, 4H), 7.24 (d, $J = 7.6$ Hz, 4H), 4.46 (s, 2H), 4.30 (br, 2H), 4.01 (br, 2H), 3.46 (br, 2H), 3.08 (br, 2H), and 1.32 (s, 18H); ^{13}C NMR (100 MHz, CDCl_3): 151.3, 150.4, 142.2, 138.4, 136.6, 132.5, 130.3, 128.8, 128.6, 125.6, 125.5, 125.3, 63.8, 54.8, 50.6, 34.72, 34.64, 31.39, and 31.32; MS (ESI) calcd for $(\text{C}_{29}\text{H}_{38}\text{NOS})^+$ $[\text{M}+\text{H}]^+$ 448.7, found 448.6.

1-(4,5-bis(4-*tert*-Butyl)phenyl)thiophen-2-yl)-*N*-methyl-*N*-(piperidin-4-ylmethyl)methanamine hydrochloride (20) was prepared from 4,5-dibromothiophene-2-carboxaldehyde, following the general method B, as a hydrochloric acid salt (white powder). ^1H NMR (400 MHz, DMSO- d_6): δ 9.58 (br, 1H), 9.02 (br, 1H), 8.85 (br, 1H), 7.53 (s, 1H), 7.38-7.35 (m, 4H), 7.24-7.20 (m, 4H), 4.55 (s, 2H), 3.27-3.24 (m, 2H), 3.05-2.99 (m, 2H), 2.90-2.84 (m, 2H), 2.77 (s, 3H), 2.17-2.10 (m, 2H), 1.98-1.95 (m, 1H), 1.46-1.39 (m, 2H), and 1.27 (s, 18H); ^{13}C NMR (100 MHz, DMSO- d_6): 150.7, 149.7, 140.4, 137.2, 136.4, 132.6, 130.4, 128.4, 128.3, 128.2, 125.7, 125.4, 58.5, 52.6, 42.42, 42.37, 34.42, 34.33, 31.14, 31.05, 28.9, and 26.4; MS (ESI) calcd for $(\text{C}_{32}\text{H}_{45}\text{N}_2\text{S})^+$ $[\text{M}+\text{H}]^+$ 489.8, found 489.6.

***N*-((4,5-bis(4-*tert*-Butyl)phenyl)thiophen-2-yl)methyl)-*N*-(piperidin-4-ylmethyl)formamide hydrochloride (21)** was prepared from 4,5-dibromothiophene-2-carboxaldehyde, following the general method B, as a hydrochloric acid salt (white powder). ^1H NMR (400 MHz, CDCl_3): δ 9.34 (br, 1H), 9.01 (br, 1H), 7.29-7.25 (m, 4H), 7.20-7.17 (m, 4H), 6.99 (s, 1H), 4.65 (s, 2H), 3.31-3.27 (m, 2H), 3.14-3.11 (m, 2H), 2.93-2.89 (m, 2H), 1.83-1.76 (m, 3H), 1.62-1.59 (m, 2H), and 1.29 (s, 18H); ^{13}C NMR (100 MHz, CDCl_3): 162.9, 154.8, 150.1, 138.7, 137.0, 136.5, 131.2, 130.8, 130.3, 128.7, 128.6, 125.5, 125.4, 52.7, 47.6, 47.5, 41.1, 34.6, 31.44, 31.36, 29.8, and 28.5; MS (ESI) calcd for $(\text{C}_{32}\text{H}_{43}\text{N}_2\text{OS})^+$ $[\text{M}+\text{H}]^+$ 503.8, found 503.6.

1-(4,5-bis(4-Isopropylphenyl)thiophen-2-yl)-*N*-(piperidin-4-ylmethyl)methanamine hydrochloride (22) was prepared from 4,5-dibromothiophene-2-carboxaldehyde, following the general method B, as a hydrochloric acid salt (white powder). ^1H NMR (400 MHz, DMSO- d_6): δ 9.67 (br, 2H), 9.13 (br, 1H), 9.03 (br, 1H), 7.50 (s, 1H), 7.20-7.15 (m, 8H), 4.34 (s, 2H), 3.26-3.23 (m, 2H), 2.90-2.83 (m, 4H), 2.75 (sep, $J = 7.0$ Hz, 2H), 2.10 (br, 1H), 1.99-1.94 (m, 2H), 1.47-1.40 (m, 2H), and 1.18 (d, $J = 7.0$ Hz, 12H); ^{13}C NMR (100 MHz, DMSO- d_6): 148.2, 147.3, 139.0, 137.1, 134.2, 133.1, 131.3, 130.9, 128.6, 128.5, 126.8, 126.5, 50.5, 44.5, 42.3, 33.1, 30.6, 28.1, 26.1, 23.8, and 23.7; MS (ESI) calcd for $(\text{C}_{29}\text{H}_{39}\text{N}_2\text{S})^+$ $[\text{M}+\text{H}]^+$ 447.7, found 447.6.

1-(4,5-bis(4-Butylphenyl)thiophen-2-yl)-*N*-(piperidin-4-ylmethyl)methanamine hydrochloride (23) was prepared from 4,5-dibromothiophene-2-carboxaldehyde, following the general method B, as a hydrochloric acid salt (white powder). ^1H NMR (400 MHz,

DMSO- d_6): δ 9.54 (br, 2H), 9.03 (br, 1H), 8.88 (br, 1H), 7.46 (s, 1H), 7.16-7.12 (m, 8H), 4.35 (s, 2H), 3.26-3.23 (m, 2H), 2.90 (br, 2H), 2.84-2.79 (m, 2H), 2.54 (t, J = 7.4 Hz, 4H), 2.09 (br, 1H), 1.97-1.93 (m, 2H), 1.52 (p, J = 7.4 Hz, 4H), 1.46-1.39 (m, 2H), 1.32-1.23 (m, 4H), and 0.87 (t, J = 7.4 Hz, 6H); ^{13}C NMR (100 MHz, DMSO- d_6): 142.5, 141.5, 139.3, 137.3, 134.2, 133.0, 131.2, 130.8, 128.86, 128.77, 128.62, 128.56, 50.7, 44.7, 42.5, 34.6, 33.09, 33.00, 30.6, 26.1, 24.8, 21.9 (2), and 13.9 (2); MS (ESI) calcd for $(\text{C}_{31}\text{H}_{43}\text{N}_2\text{S})^+ [\text{M} + \text{H}]^+$ 475.8, found 475.7.

1-(5-(4-(*tert*-Butyl)phenyl)-4-(furan-3-yl)phenyl)thiophen-2-yl)-*N*-(piperidin-4-ylmethyl)methanamine hydrochloride (24) was prepared from 4,5-dibromothiophene-2-carboxaldehyde, following the general method B, as a hydrochloric acid salt (white powder). ^1H NMR (400 MHz, DMSO- d_6): δ 9.51 (br, 2H), 8.95 (br, 1H), 8.79 (br, 1H), 8.08 (s, 1H), 7.89 (d, J = 8.1 Hz, 1H), 7.61-7.58 (m, 1H), 7.52 (s, 1H), 7.39-7.36 (m, 2H), 7.32 (d, J = 8.1 Hz, 1H), 7.24-7.19 (m, 4H), 6.97 (s, 1H), 4.38 (s, 2H), 3.28-3.25 (m, 2H), 2.93-2.88 (m, 2H), 2.86-2.82 (m, 2H), 2.08 (br, 1H), 1.98-1.95 (m, 2H), 1.47-1.42 (m, 2H), and 1.26 (s, 9H); ^{13}C NMR (100 MHz, DMSO- d_6): 146.5, 144.5, 139.6, 136.7, 134.1, 133.9, 131.6, 131.4, 129.0, 128.8, 128.4, 128.3, 127.4, 125.8, 125.7, 108.5, 50.6, 44.6, 42.4, 34.4, 31.0, 30.5, and 26.1; MS (ESI) calcd for $(\text{C}_{31}\text{H}_{37}\text{N}_2\text{OS})^+ [\text{M} + \text{H}]^+$ 485.7, found 485.6.

1-(4-(4-(Furan-3-yl)phenyl)-5-(4-(piperidin-1-ylmethyl)phenyl)thiophen-2-yl)-*N*-(piperidin-4-ylmethyl)methanamine hydrochloride (25) was prepared from 4,5-dibromothiophene-2-carboxaldehyde, following the general method B, as a hydrochloric acid salt (white powder). ^1H NMR (400 MHz, DMSO- d_6): δ 10.50 (br, 1H), 9.60 (br, 2H), 8.91 (br, 1H), 8.78 (br, 1H), 8.21 (s, 1H), 7.75 (s, 1H), 7.64-7.54 (m, 5H), 7.35 (d, J = 8.1 Hz, 2H), 7.24 (d, J = 8.1 Hz, 2H), 6.97 (s, 1H), 4.40 (s, 2H), 4.24 (s, 2H), 3.28-3.24 (m, 4H), 2.94-2.90 (m, 2H), 2.86-2.81 (m, 4H), 2.09 (br, 1H), 1.98-1.95 (m, 2H), 1.77 (br, 4H), 1.71-1.67 (m, 2H), and 1.48-1.39 (m, 2H); ^{13}C NMR (100 MHz, DMSO- d_6): 144.5, 139.6, 138.4, 137.6, 134.4, 134.1, 133.7, 132.1, 132.0, 131.5, 131.4, 129.0, 128.8, 128.7, 125.8, 108.6, 51.6, 50.6, 44.5, 42.3, 30.7, 30.5, 26.1, 22.1, and 21.4; MS (ESI) calcd for $(\text{C}_{33}\text{H}_{40}\text{N}_3\text{OS})^+ [\text{M} + \text{H}]^+$ 526.8, found 526.6.

1-(5-(4-(Aminomethyl)phenyl)-4-(4-(*tert*-butyl)phenyl)thiophen-2-yl)-*N*-(piperidin-4-ylmethyl)methanamine hydrochloride (26) was prepared from 4,5-dibromothiophene-2-carboxaldehyde, following the general method B, as a hydrochloric acid salt (white powder). ^1H NMR (400 MHz, D_2O): δ 7.63 (s, 1H), 7.45 (d, J = 9.2 Hz, 2H), 7.42-7.39 (m, 4H), 7.28 (d, J = 9.2 Hz, 2H), 4.54 (s, 2H), 4.18 (s, 2H), 3.50-3.46 (m, 2H), 3.14 (br, 2H), 3.03 (t, J = 14.4 Hz, 2H), 2.15 (br, 1H), 2.07-2.04 (m, 2H), 1.57-1.48 (m, 2H), and 1.29 (s, 9H); ^{13}C NMR (100 MHz, D_2O): 144.2, 139.8, 138.3, 137.4, 134.0, 132.4, 130.2, 129.8, 129.1, 128.7, 125.6, 108.8, 50.7, 44.4, 43.1, 42.6, 30.7, 30.3, 25.8, and 22.1; MS (ESI) calcd for $(\text{C}_{28}\text{H}_{38}\text{N}_3\text{S})^+ [\text{M} + \text{H}]^+$ 448.7, found 448.8.

1-(4-(4-(Aminomethyl)phenyl)-5-(4-(*tert*-butyl)phenyl)thiophen-2-yl)-*N*-(piperidin-4-ylmethyl)-methanamine hydrochloride (27) was prepared from 4,5-dibromothiophene-2-carboxaldehyde, following the general method B, as a hydrochloric acid salt (white powder). ^1H NMR (400 MHz, DMSO- d_6): δ 9.73 (br, 1H), 9.12 (br, 1H), 9.00 (br, 1H), 8.50 (br, 2H), 8.28 (br, 2H), 7.55 (s, 1H), 7.47 (d, J = 7.9 Hz, 2H), 7.37 (d, J = 7.9 Hz, 2H), 7.28 (d, J = 7.9

Hz, 2H), 7.19 (d, $J = 7.9$ Hz, 2H), 4.35 (s, 2H), 4.00 (s, 2H), 3.24 (d, $J = 12.7$ Hz, 2H), 2.89-2.83 (m, 4H), 2.10 (br, 1H), 1.97 (d, $J = 12.3$ Hz, 2H), 1.50-1.42 (m, 2H), and 1.27 (s, 9H); ^{13}C NMR (100 MHz, DMSO- d^6): 150.7, 139.6, 136.6, 135.7, 134.2, 133.0, 130.5, 129.2, 128.7, 128.4, 125.7, 115.3, 50.5, 44.4, 42.3, 41.8, 34.4, 31.0, 30.5, and 26.1; MS (ESI) calcd for $(\text{C}_{28}\text{H}_{38}\text{N}_3\text{S})^+ [\text{M}+\text{H}]^+$ 448.7, found 448.8.

((5-((Piperidin-4-ylmethyl)amino)methyl)thiophene-2,3-diyl)bis(4,1-phenylene)dimethanamine hydrochloride (28) was prepared from 4,5-dibromothiophene-2-carboxaldehyde, following the general method B, as a hydrochloric acid salt (white powder). ^1H NMR (400 MHz, D_2O) δ 7.43 (s, 1H), 7.40 (br, 8H), 4.57 (s, 2H), 4.19 (s, 4H), 3.50 (d, $J = 12.8$ Hz, 2H), 3.15 (d, $J = 6.8$ Hz, 2H), 3.05 (t, $J = 12.0$ Hz, 2H), 2.18 (s, 1H), 2.08 (d, $J = 14.0$ Hz, 2H), and 1.59-1.50 (m, 2H); ^{13}C NMR (100 MHz, D_2O) 140.6, 137.9, 136.1, 133.9, 133.8, 132.6, 131.8, 130.5, 129.9, 129.6, 129.1, 129.0, 50.8, 45.4, 43.1, 42.64, 42.57, 30.7, and 25.8. MS (ESI) calcd for $(\text{C}_{25}\text{H}_{33}\text{N}_4\text{S})^+ [\text{M}+\text{H}]^+$ 421.6, found 421.5.

((5-((Piperidin-4-ylmethyl)amino)methyl)thiophene-2,3-diyl)bis(4,1-phenylene)dimethanol hydrochloride (29) was prepared from 4,5-dibromothiophene-2-carboxaldehyde, following the general method B, as a hydrochloric acid salt (white powder). ^1H NMR (400 MHz, DMSO- d^6): δ 9.42 (br, 2H), 8.91 (br, 1H), 8.74 (br, 1H), 7.47 (s, 1H), 7.28 (d, $J = 7.1$ Hz, 2H), 7.26 (d, $J = 7.1$ Hz, 2H), 7.19 (d, $J = 7.1$ Hz, 2H), 7.17 (d, $J = 7.1$ Hz, 2H), 4.47 (s, 4H), 4.37 (s, 2H), 3.27-3.24 (m, 2H), 2.92 (br, 2H), 2.89-2.82 (m, 2H), 2.07 (br, 1H), 1.97-1.93 (m, 2H), and 1.48-1.39 (m, 2H); ^{13}C NMR (100 MHz, DMSO- d^6): 142.6, 141.7, 139.5, 137.4, 134.2, 134.0, 131.8, 131.4, 128.7, 128.4, 127.0, 126.8, 62.7, 62.6, 50.8, 44.8, 42.5, 30.6, and 26.1; MS (ESI) calcd for $(\text{C}_{25}\text{H}_{31}\text{N}_2\text{O}_2\text{S})^+ [\text{M}+\text{H}]^+$ 423.6, found 423.5.

1-(4,5-di(Furan-3-yl)thiophen-2-yl)-N-(piperidin-4-ylmethyl)methanamine hydrochloride (30) was prepared from 4,5-dibromothiophene-2-carboxaldehyde, following the general method B, as a hydrochloric acid salt (white powder). ^1H NMR (400 MHz, DMSO- d^6): δ 9.61 (br, 2H), 9.09 (br, 1H), 8.96 (br, 1H), 7.88 (s, 1H), 7.78 (s, 2H), 7.71 (s, 1H), 7.48 (s, 1H), 6.52 (s, 1H), 6.48 (s, 1H), 4.32 (s, 2H), 3.27-3.24 (m, 2H), 2.87-2.82 (m, 4H), 2.08 (br, 1H), 1.97-1.94 (m, 2H), and 1.45-1.40 (m, 2H); ^{13}C NMR (100 MHz, DMSO- d^6): 144.2, 143.7, 140.9, 140.2, 133.1, 131.1, 129.8, 129.2, 120.1, 118.1, 111.1, 110.3, 50.4, 44.4, 42.3, 30.5, and 26.0; MS (ESI) calcd for $(\text{C}_{19}\text{H}_{23}\text{N}_2\text{O}_2\text{S})^+ [\text{M}+\text{H}]^+$ 343.5, found 343.4.

1-(4,5-bis(3,4-Dimethoxyphenyl)thiophen-2-yl)-N-(piperidin-4-ylmethyl)methanamine hydrochloride (31) was prepared from 4,5-dibromothiophene-2-carboxaldehyde, following the general method B, as a hydrochloric acid salt (white powder). ^1H NMR (400 MHz, DMSO- d^6): δ 9.40 (br, 2H), 8.94 (br, 1H), 8.77 (br, 1H), 7.47 (s, 1H), 7.17-7.14 (m, 1H), 7.01-6.91 (m, 2H), 6.84 (d, $J = 8.4$ Hz, 1H), 6.78 (s, 1H), 6.74 (s, 1H), 4.34 (s, 2H), 3.75 (s, 3H), 3.73 (s, 3H), 3.56 (s, 3H), 3.54 (s, 3H), 3.28-3.25 (m, 2H), 2.92 (br, 2H), 2.88-2.82 (m, 2H), 2.07 (br, 1H), 1.98-1.91 (m, 2H), and 1.48-1.38 (m, 2H); ^{13}C NMR (100 MHz, DMSO- d^6): 148.8, 148.51, 148.48, 148.1, 136.9, 131.6, 131.5, 128.9, 128.8, 125.9, 121.4, 121.0, 112.54, 112.52, 112.0, 111.9, 55.69, 55.62, 55.59, 55.36, 50.7, 44.8, 42.4, 30.6, and 26.1; MS (ESI) calcd for $(\text{C}_{27}\text{H}_{35}\text{N}_2\text{O}_4\text{S})^+ [\text{M}+\text{H}]^+$ 483.6, found 483.5.

1-(4,5-di([1,1'-Biphenyl]-3-yl)thiophen-2-yl)-N-(piperidin-4-ylmethyl)methanamine hydrochloride (32) was prepared from 4,5-dibromothiophene-2-carboxaldehyde, following the general method B, as a hydrochloric acid salt (white powder). ¹H NMR (400 MHz, DMSO-d⁶): δ 9.50 (br, 2H), 8.88 (br, 1H), 8.68 (br, 1H), 7.65 (s, 2H), 7.52-7.31 (m, 17H), 4.42 (s, 2H), 3.29-3.26 (m, 2H), 2.95 (br, 2H), 2.90-2.82 (m, 2H), 2.08 (br, 1H), 1.98-1.95 (m, 2H), and 1.48-1.39 (m, 2H); ¹³C NMR (100 MHz, DMSO-d⁶): 140.7, 140.5, 139.8, 139.5, 139.4, 137.6, 136.0, 133.9, 129.7, 129.4, 128.95 (2), 128.90 (2), 127.9, 127.7, 127.6 (2), 127.24, 127.17, 126.6 (2), 126.5, 125.8, 50.5, 44.5, 42.3, 30.5, and 26.1; MS (ESI) calcd for (C₃₅H₃₅N₂S)⁺ [M+H]⁺ 515.7, found 515.5.

1-(3-Bromo-4,5-bis(4-(tert-butyl)phenyl)thiophen-2-yl)-N-(piperidin-4-ylmethyl)methanamine hydrochloride (33) was prepared from 4,5-dibromothiophene-2-carboxaldehyde, following the general method B, as a hydrochloric acid salt (white powder). ¹H NMR (400 MHz, DMSO-d⁶): δ 9.65 (br, 1H), 9.00 (br, 1H), 8.84 (br, 1H), 8.10 (br, 1H), 7.44 (d, *J* = 8.2 Hz, 2H), 7.31 (d, *J* = 8.2 Hz, 2H), 7.14 (d, *J* = 8.2 Hz, 2H), 7.11 (d, *J* = 8.2 Hz, 2H), 4.41 (s, 2H), 3.28-3.25 (m, 2H), 2.97 (br, 2H), 2.89-2.82 (m, 2H), 2.09 (br, 1H), 1.99-1.96 (m, 2H), 1.49-1.43 (m, 2H), 1.30 (s, 9H), and 1.22 (s, 9H); ¹³C NMR (100 MHz, DMSO-d⁶): 151.1, 150.4, 141.2, 137.0, 132.0, 129.95, 129.84, 128.0, 126.6, 125.6, 125.3, 118.0, 50.9, 44.7, 43.0, 42.3, 34.44, 34.40, 31.1, 30.9, and 26.0; MS (ESI) calcd for (C₃₁H₄₂BrN₂S)⁺ [M+H]⁺ 554.7, found 554.6.

1-(4,5-bis(4-(tert-Butyl)phenyl)furan-2-yl)-N-(piperidin-4-ylmethyl)methanamine hydrochloride (34) was prepared from 4,5-dibromofuran-2-carboxaldehyde, following the general method B, as a hydrochloric acid salt (white powder). ¹H NMR (400 MHz, DMSO-d⁶): δ 9.54 (br, 2H), 8.97 (br, 1H), 8.78 (br, 1H), 7.46-7.33 (m, 8H), 6.88 (s, 1H), 4.28 (s, 2H), 3.28-3.25 (m, 2H), 2.94 (br, 2H), 2.85-2.83 (m, 2H), 2.06 (br, 1H), 1.97-1.94 (br, 2H), 1.48-1.42 (m, 2H), 1.30 (s, 9H), and 1.27 (s, 9H); ¹³C NMR (100 MHz, DMSO-d⁶): 150.9, 150.0, 148.4, 144.8, 130.2, 127.8, 127.5, 125.8, 125.7, 125.5, 122.2, 116.2, 50.7, 42.8, 42.4, 34.49, 34.39, 31.15, 31.02, 30.5 and 26.0; MS (ESI) calcd for (C₃₁H₄₃N₂O)⁺ [M+H]⁺ 459.7, found 459.6.

1-(4,5-bis(4-(Furan-3-yl)phenyl)furan-2-yl)-N-(piperidin-4-ylmethyl)methanamine hydrochloride (35) was prepared from 4,5-dibromofuran-2-carboxaldehyde, following the general method B, as a hydrochloric acid salt (yellow powder). ¹H NMR (400 MHz, DMSO-d⁶): δ 9.57 (br, 2H), 8.96 (br, 1H), 8.78 (br, 1H), 8.24-8.21 (m, 1H), 7.78-7.74 (m, 2H), 7.70-7.58 (m, 5H), 7.55 (d, *J* = 8.0 Hz, 2H), 7.41 (d, *J* = 8.0 Hz, 2H), 6.99 (s, 1H), 6.96 (d, *J* = 8.0 Hz, 2H), 4.31 (s, 2H), 3.27-3.23 (m, 2H), 2.95 (br, 2H), 2.89-2.83 (m, 2H), 2.08 (br, 1H), 1.98-1.92 (m, 2H), and 1.49-1.38 (m, 2H); ¹³C NMR (100 MHz, DMSO-d⁶): 148.5, 145.2, 144.6, 139.9, 139.7, 131.6, 131.5, 128.9, 128.8, 128.7, 126.6, 126.1, 125.8, 125.4, 124.3, 122.6, 116.1, 114.7, 108.67, 108.61, 50.7, 42.9, 42.4, 30.6, and 26.1; MS (ESI) calcd for (C₃₁H₃₁N₂O₃)⁺ [M+H]⁺ 479.6, found 479.5.

4,5-bis(4-(tert-Butyl)phenyl)-N-(piperidin-4-ylmethyl)thiazole-2-carboxamide hydrochloride (36) was prepared from 4-bromothiazole-2-carboxaldehyde, following the general method A, as a hydrochloric acid salt (white powder). ¹H NMR (400 MHz, DMSO-d⁶): δ 8.96 (br, 1H), 8.85 (br, 1H), 8.53 (br, 1H), 7.48-7.42 (m, 4H), 7.38-7.33 (m, 4H),

3.26-3.20 (m, 4H), 2.82 (br, 2H), 1.87 (br, 1H), 1.82-1.76 (m, 2H), 1.42-1.36 (m, 2H), and 1.28 (s, 18H); ^{13}C NMR (100 MHz, DMSO- d_6): 161.0, 152.1, 151.3, 150.4, 137.8, 137.5, 131.7, 129.4, 128.9, 128.3, 126.4, 125.6, 44.2, 43.2, 34.9, 34.8, 34.1, 31.5, 31.4, and 26.6; MS (ESI) calcd for $(\text{C}_{30}\text{H}_{40}\text{N}_3\text{OS})^+ [\text{M}+\text{H}]^+$ 490.7, found 490.6.

1-(4,5-bis(4-(*tert*-Butyl)phenyl)thiazol-2-yl)-*N*-(piperidin-4-ylmethyl)methanamine hydrochloride (37) was prepared from 4-bromothiazole-2-carboxaldehyde, following the general method B, as a hydrochloric acid salt (white powder). ^1H NMR (400 MHz, DMSO- d_6): δ 9.83 (br, 2H), 9.13 (br, 1H), 8.98 (br, 1H), 7.44-7.31 (m, 8H), 4.57 (s, 2H), 3.27-3.24 (m, 2H), 3.03 (br, 2H), 2.85 (br, 2H), 2.10 (br, 1H), 1.98-1.95 (m, 2H), 1.55-1.50 (m, 2H), and 1.27 (s, 18H); ^{13}C NMR (100 MHz, DMSO- d_6): 151.4, 150.6, 148.5, 134.2, 131.7, 131.3, 129.0, 128.2, 128.0, 126.0, 125.2, 51.3, 46.8, 42.3, 34.52, 34.42, 31.07, 31.02, 30.6, and 28.1; MS (ESI) calcd for $(\text{C}_{30}\text{H}_{42}\text{N}_3\text{S})^+ [\text{M}+\text{H}]^+$ 476.7, found 476.5.

1-(4-(4-(*tert*-Butyl)phenyl)thiazol-2-yl)-*N*-(piperidin-4-ylmethyl)methanamine hydrochloride (38) was prepared from 4-bromothiazole-2-carboxaldehyde, following the general method B, as a hydrochloric acid salt (white powder). ^1H NMR (400 MHz, DMSO- d_6): δ 9.77 (br, 2H), 9.01 (br, 2H), 8.01 (s, 1H), 7.86 (d, $J = 8.4$ Hz, 2H), 7.42 (d, $J = 8.4$ Hz, 2H), 4.55 (s, 2H), 3.27-3.24 (m, 2H), 3.03 (br, 2H), 2.85 (br, 2H), 2.10 (br, 1H), 1.98-1.95 (m, 2H), 1.47-1.39 (m, 2H), and 1.25 (s, 9H); ^{13}C NMR (100 MHz, DMSO- d_6): 160.0, 154.3, 150.9, 131.0, 125.9, 125.6, 116.0, 51.2, 46.8, 42.3, 34.4, 31.1, 30.6, and 26.0; MS (ESI) calcd for $(\text{C}_{20}\text{H}_{30}\text{N}_3\text{S})^+ [\text{M}+\text{H}]^+$ 344.5, found 344.6.

4-(4-(*tert*-Butyl)phenyl)-*N*-(piperidin-4-ylmethyl)thiazole-2-carboxamide hydrochloride (39) was prepared from 4-bromothiazole-2-carboxaldehyde, following the general method A, as a hydrochloric acid salt (white powder). ^1H NMR (400 MHz, DMSO- d_6): δ 8.99 (br, 1H), 8.90 (br, 1H), 8.68 (br, 1H), 8.34 (s, 1H), 7.98 (d, $J = 8.2$ Hz, 2H), 7.49 (d, $J = 8.2$ Hz, 2H), 3.27-3.19 (m, 4H), 2.88-2.79 (m, 2H), 1.91 (br, 1H), 1.83-1.79 (m, 2H), 1.67-1.63 (m, 2H), and 1.31 (s, 9H); ^{13}C NMR (100 MHz, DMSO- d_6): 163.5, 159.4, 153.9, 151.2, 130.8, 126.1, 125.5, 118.8, 43.8, 42.9, 34.4, 31.1, 28.1, and 26.3; MS (ESI) calcd for $(\text{C}_{20}\text{H}_{28}\text{N}_3\text{OS})^+ [\text{M}+\text{H}]^+$ 358.5, found 358.4.

***N*-((5,6-bis(4-(Furan-3-yl)phenyl)pyrazin-2-yl)methyl)piperidin-4-amine hydrochloride (40).**

A mixture of 2,3-diaminopropanoic acid hydrochloride (600.4 mg, 4.26 mmol), 1,2-bis(4-bromophenyl)ethane-1,2-dione **52** (1.745 g, 4.26 mmol) and NaOH (677.2 mg, 16.93 mmol) in methanol (25 mL) were refluxed for 2 h. The mixture was cooled to 25°C and air was bubbled through the solution for 2 days, after which pH was adjusted to 2 by HCl. Upon removal of the solvents, the product was extracted with diethyl ether (3 × 50 mL) and the combined organic phases were dried, filtered and evaporated under reduced pressure. The crude product **53** was dissolved in THF (22 mL) followed by addition of methyl chloroformate (0.22 mL, 2.8 mmol) and diisopropylethylamine (0.6 mL, 3.5 mmol). The reaction mixture was stirred at room temperature for 5h. Methanol (1.8 mL) was then added followed by NaBH₄ (537.2 mg, 14.2 mmol) in small portions at 0°C. Stirring was continued at 0°C for 1h. The product was extracted with ether and purified with flash chromatography (silica gel, hexane/ethyl acetate = 5/1) to give the corresponding alcohol (509 mg, 52% for two steps), which was converted to compound **40** as a pale yellow powder using the

reactions vi, vii, ii and iv described in general methods A and B. ^1H NMR (400 MHz, DMSO- d_6): δ 8.94 (br, 2H), 8.72 (br, 1H), 8.69 (s, 1H), 8.24 (br, 2H), 7.92 (d, $J = 7.1$ Hz, 2H), 7.75 (s, 2H), 7.62 (d, $J = 7.7$ Hz, 4H), 7.45 (d, $J = 4.5$ Hz, 2H), 7.43 (d, $J = 4.5$ Hz, 2H), 6.99 (s, 2H), 5.26 (s, 2H), 3.21 (d, $J = 10.2$ Hz, 2H), 2.94 (br, 2H), 2.79-2.75 (m, 2H), 1.76 (d, $J = 14.2$ Hz, 2H), 1.69 (br, 1H), and 1.33-1.26 (m, 2H); ^{13}C NMR (100 MHz, DMSO- d_6): 156.0, 150.48, 150.44, 149.5, 144.5, 140.4, 140.02, 139.99, 136.63, 136.57, 132.3, 130.1, 130.0, 129.7, 128.0, 126.4, 125.3, 125.2, 108.58, 108.56, 53.4, 45.3, 42.7, 33.9, and 26.0; MS (ESI) calcd for $(\text{C}_{31}\text{H}_{31}\text{N}_4\text{O}_2)^+ [\text{M}+\text{H}]^+$ 491.6, found 491.5.

Inhibition of p300-HAT and other HATs.

The HAT domain (1195-1673) of human p300 was cloned, inserted into pGEX-KG vector and the DNA sequence was verified by sequencing. The p300-HAT expression plasmid was transformed into *E. coli* BL21-CodonPlus strain (Agilent) and cultured at 37 °C in LB medium containing ampicillin (50 $\mu\text{g}/\text{mL}$) and chloramphenicol (34 $\mu\text{g}/\text{mL}$). After the optical density of the bacterial culture reached ~ 0.9 at 600 nm, p300 HAT expression was induced by adding 300 μM isopropylthiogalactoside (IPTG) at 18 °C for 48 hours. Cells were collected, lysed, centrifuged for 20 min at 20,000 rpm. The supernatant was subjected to column chromatography with glutathione sepharose resins. The recombinant GST-p300-HAT fusion protein was obtained in $\sim 90\%$ purity (SDS-PAGE) by elution with 10 mM of glutathione solution, which was further purified using a Superdex 200 gel filtration column chromatography. CBP, PCAF and Myst3 HATs were obtained using similar methods.

To determine inhibitory activity, a compound with concentrations ranging from 100 nM to 10 μM was incubated with p300-HAT (10 nM) in 20 μL of 50 mM phosphate buffer (pH = 7.0) containing 0.01% Brij-35 for 10 min at 25 °C. Histone H3 peptide (ARTKQTARKSTGGKAPRKQLA) (20 μM) and Acetyl-CoA (1 μM ^3H -Ac-CoA and 19 μM Ac-CoA) were added to initiate the reaction. After 30 min at 25 °C, the reaction was stopped by adding 6 N formic acid (5 μL). 20 μL of reaction mixture was then transferred to a small piece of P81 filter paper (Whatman) that binds histone H3 peptide. The filter paper was washed 3x with 50 mM NaHCO_3 , dried, and transferred into a scintillation vial containing 2 mL of scintillation cocktail. Radioactivity on the filter paper was measured with a Beckman LS-6500 scintillation counter. IC_{50} values were obtained by using a standard sigmoidal dose response curve fitting in Prism (version 5.0, GraphPad Software, Inc., La Jolla, CA). IC_{50} values were the mean values from at least three experiments.

Alpha assay.

We followed a published method¹⁶ to investigate whether compound **2** can disrupt the binding of p300 HAT and histone H4 peptide. In brief, the assay was performed in a 384-well plate using His6-tagged P300 HAT (125 nM) coated nickel chelate acceptor beads (5 μL , Perkin Elmer), biotinylated H4 peptide [SGRGKGGKGLGKGGAKRHRKVLRRGK(Biotin)-NH₂] (30 nM) coated streptavidin donor beads (5 μL , Perkin Elmer), and varying concentrations of **12** in a PBS buffer with 0.5 % BSA (final volume of 25 μL). Upon incubation for 1h, Alpha signal was determined (laser excitations at 680 nm and reading at 570 nm) using a Tecan Spark microplate reader. The IC_{50} values were determined using the sigmoidal dose-response fitting in the program of Prism 5.0 (GraphPad). The biotinylated

His6 peptide (Perkin Elmer # 6760302) was used as a reference to eliminate the possible interference of compounds on the signal generated by singlet oxygen transfer.

Molecular modeling.

Docking studies were performed with Schrödinger small-molecule drug discovery software suite (Schrödinger, LLC, New York, NY, 2017), using our previous published methods^{23, 35}. The crystal structure of p300-HAT in complex with Ac-CoA (PDB: 4PZS) was prepared using the module “protein preparation wizard” in Maestro with the default protein parameters. Hydrogen atoms were added and water molecules were extracted. Ac-CoA was included in the protein structure for docking. Hydrogen bonds were optimized, the partial charges were assigned, and the protein structure was energy-minimized using OPLS-2005 force field. A receptor grid was generated using the program Glide without any constraints. Compound **12** was constructed, energy-minimized using OPLS-2005 force field in Maestro and then docked into the prepared protein structure using Glide (docking parameters: standard-precision and dock flexibly).

Western blot.

10⁶ Kasumi-1 cells/well were incubated with compound **12** at 0, 5 and 10 μM for 12 hours. Histone proteins were extracted using EpiQuik total histone extraction kit (Epigentek), according to the manufacturer’s protocol. Equal amounts of histones (2 μg) were separated on SDS-PAGE and transferred to PVDF membranes. The blots were probed with primary antibodies against H3K9Ac, H3K18Ac, H3K27Ac and H3 (Cell Signaling), followed by anti-rabbit IgG (Thermo Scientific) secondary antibodies.

Cell growth inhibition.

The anti-proliferation assays for non-breast cancer cells were performed using our previous method³⁶⁻³⁸. In brief, for Kasumi-1 cells, 10⁶ cells per well were added into 96-well plates and cultured with increasing concentrations of a compound in RPMI-1640 medium supplemented with 20% fetal bovine serum and penicillin (100 U/mL) and streptomycin (100 μg/mL) at 37 °C in a 5% CO₂ atmosphere with 100% humidity. For solid tumor cells, 10⁵ cells per well were added into 96-well plates and cultured in Dulbecco’s Modified Eagle’s Medium (DMEM) supplemented with 10% fetal bovine serum and penicillin (100 U/mL) and streptomycin (100 μg/mL) overnight. Upon addition of increasing concentrations of a compound, cells were incubated for 5 days. Cell viability was assessed by using an XTT assay kit (Roche) for leukemia cells or an MTT assay (Sigma) for attachment cells. For the breast cancer MCF-7 cells, culture and inhibition assays were performed according to our previous methods^{28, 29}. Compound EC₅₀ values were calculated from dose response curves using Prism 5.0.

RNA extraction.

Upon starvation (culturing in phenol red-free DMEM medium with 10% charcoal treated FBS to remove hydrophobic hormones such as estrogens) for 7 days, MCF-7 cells were treated with the p300 inhibitor (6 μM) or DMSO control, in the presence or absence of (10

nM) estradiol (E2) for 48 hours. Total RNA was extracted using RNeasy Plus Mini Kit (Qiagen), according to the manufacturer's instruction.

Library Preparation.

The RNA integrity for each sample was assessed with a RNA 6000 Nano chip on a 2100 Bioanalyzer (Agilent; Santa Clara, CA). The average RNA integrity score for the sample set was 6.48. Sequencing libraries were prepared using the TruSeq Stranded Total RNA Library Prep Kit (Illumina, Inc; San Diego, CA). Concisely, ribosomal RNA (rRNA) was depleted from total RNA where the remaining (ribo-depleted RNA) was purified, fragmented for 7.5 minutes, and primed for cDNA synthesis. Blunt-ended cDNA was generated after first and second strand synthesis. Adenylation of the 3' blunt-ends was followed by adapter ligation prior to the enrichment of the cDNA fragments. Final library quality control was carried out by measuring the fragment size on a DNA1000 chip on a 2100 BioAnalyzer (Agilent; Santa Clara, CA). The average library yielded an insert bp size of 258. The concentration of each library was determined by quantitative PCR (qPCR) by the KAPA Library Quantification Kit for Next Generation Sequencing (KAPA Biosystems; Woburn, MA).

Sequencing.

Libraries were normalized to 50 nmol/L in 10 mM Tris-Cl, pH8.5 with 0.1% Tween 20 then pooled evenly. The 50 nmol/L library pool was diluted to 2 nmol/L with 10 mM Tris-Cl, pH8.5 with 0.1% Tween 20. The pooled libraries were denatured with 0.05N NaOH and diluted to 20 pmol/L. Cluster generation of the denatured libraries was performed according to the manufacture's specifications (Illumina, Inc; San Diego, CA) utilizing the HiSeq Rapid PE Cluster Kit v2 chemistry and flow cell. Libraries were clustered appropriately with a 1% PhiX spike-in. Sequencing-by-synthesis (SBS) was performed on a HiSeq 2500 utilizing v2 chemistry with paired-end 101 bp reads and a 6 bp index read culminating in an average output of 20 million paired-end reads (or 40 million total reads) per sample. Sequence read data were processed and converted to FASTQ format by Illumina BaseSpace analysis software (v2.0.13).

Bioinformatics Analysis.

RNAseq data files were trimmed using Trim Galore! ^{39, 40}. Then the data was mapped using Hisat2 onto the human reference genome build UCSC hg38/GRCh38 and sorted using samtools ^{41, 42}. Gene expression was assessed and fragments per kilobase of transcript per million (FPKM) values were determined using Stringtie ⁴¹. Gene expression profiles were normalized using the quantile normalization method. Significantly changed genes were determined using a two-sided parametric t-test, with significance assessed at $p < 0.05$, only genes for which at least one sample exceeded 1 FPKM in expression were considered. Enriched pathways were inferred using the Gene Set Enrichment (GSEA) method, and the Molecular Signature Database (MSigDB) pathway collection.

Supplementary Material

Refer to Web version on PubMed Central for supplementary material.

Acknowledgment.

This work was supported by the Cancer Prevention and Research Institute of Texas (CPRIT) grants RP150129 and RP180177 to Y.S. It was also partly supported in part by the Breast Cancer Research Foundation grants 16-142; 17-143 ,18-145 (to R.S.), Susan G. Komen for the Cure Foundation Promise Grants (PG12221410 to R.S.), Department of Defense (W81XWH-14-1-0326 to X.F.), and the NCI SPORE P50CA58183 and P50CA186784 grants (to R.S. and N.M.). The gene expression profiling was supported by the CPRIT grant RP170005, the Prostate Cancer Foundation Grant 18YOUN09 to (S.K.) and NCI SPORE P50 CA186784 (N.M.). The authors also acknowledge the assistance of the Dan L Duncan Cancer Center Core resources (supported by the NCI Cancer Center Support Grant P30CA125123).

ABBREVIATIONS:

Ac-CoA	acetyl coenzyme A
AR	androgen receptor
CBP	CREB (cAMP-response element binding protein) binding protein
CH1	cysteine-histidine rich 1
CoA	coenzyme A
ER	estrogen receptor
GNAT	Gcn5-related N-acetyltransferase
GSEA	Gene set enrichment analysis
H3K4	Histone H3 lysine 4
H3K9	Histone H3 lysine 9
H3K27	Histone H3 lysine 27
LSD1	lysine specific demethylase 1
MYST	MOZ, Ybf2, Sas2 and Tip60p300
NES	normalized enrichment score
E1A	binding protein p300
PCAF	p300/CBP associating factor
SAR	structure activity relationship
SID	steroid receptor coactivator interaction
SRC	steroid receptor coactivator

References

1. Jones PA; Baylin SB The epigenomics of cancer. *Cell* 2007, 128, 683–692. [PubMed: 17320506]
2. Kouzarides T Chromatin modifications and their function. *Cell* 2007, 128, 693–705. [PubMed: 17320507]

3. Belkina AC; Denis GV BET domain co-regulators in obesity, inflammation and cancer. *Nat Rev Cancer* 2012, 12, 465–477. [PubMed: 22722403]
4. Yang Z; Yik JH; Chen R; He N; Jang MK; Ozato K; Zhou Q Recruitment of P-TEFb for stimulation of transcriptional elongation by the bromodomain protein Brd4. *Mol Cell* 2005, 19, 535–545. [PubMed: 16109377]
5. Schiltz RL; Mizzen CA; Vassilev A; Cook RG; Allis CD; Nakatani Y Overlapping but distinct patterns of histone acetylation by the human coactivators p300 and PCAF within nucleosomal substrates. *J Biol Chem* 1999, 274, 1189–1192. [PubMed: 9880483]
6. Dancy BM; Cole PA Protein lysine acetylation by p300/CBP. *Chem Rev* 2015, 115, 2419–2452. [PubMed: 25594381]
7. Wang F; Marshall CB; Ikura M Transcriptional/epigenetic regulator CBP/p300 in tumorigenesis: structural and functional versatility in target recognition. *Cell Mol Life Sci* 2013, 70, 3989–4008. [PubMed: 23307074]
8. Johnson AB; O'Malley BW Steroid receptor coactivators 1, 2, and 3: critical regulators of nuclear receptor activity and steroid receptor modulator (SRM)-based cancer therapy. *Mol Cell Endocrinol* 2012, 348, 430–439. [PubMed: 21664237]
9. Dilworth FJ; Chambon P Nuclear receptors coordinate the activities of chromatin remodeling complexes and coactivators to facilitate initiation of transcription. *Oncogene* 2001, 20, 3047–3054. [PubMed: 11420720]
10. Kraus WL; Manning ET; Kadonaga JT Biochemical analysis of distinct activation functions in p300 that enhance transcription initiation with chromatin templates. *Mol Cell Biol* 1999, 19, 8123–8135. [PubMed: 10567538]
11. Gu W; Shi XL; Roeder RG Synergistic activation of transcription by CBP and p53. *Nature* 1997, 387, 819–823. [PubMed: 9194564]
12. Vervoorts J; Luscher-Firzlaff JM; Rottmann S; Lilischkis R; Walsemann G; Dohmann K; Austen M; Luscher B Stimulation of c-MYC transcriptional activity and acetylation by recruitment of the cofactor CBP. *EMBO Rep* 2003, 4, 484–490. [PubMed: 12776737]
13. Ma H; Hong H; Huang SM; Irvine RA; Webb P; Kushner PJ; Coetzee GA; Stallcup MR Multiple signal input and output domains of the 160-kilodalton nuclear receptor coactivator proteins. *Mol Cell Biol* 1999, 19, 6164–6173. [PubMed: 10454563]
14. Lavau C; Du C; Thirman M; Zeleznik-Le N Chromatin-related properties of CBP fused to MLL generate a myelodysplastic-like syndrome that evolves into myeloid leukemia. *EMBO J* 2000, 19, 4655–4664. [PubMed: 10970858]
15. Gervais C; Murati A; Helias C; Struski S; Eischen A; Lippert E; Tigaud I; Penther D; Bastard C; Mugneret F; Poppe B; Speleman F; Talmant P; VanDen Akker J; Baranger L; Barin C; Luquet I; Nadal N; Nguyen-Khac F; Maarek O; Herens C; Sainy D; Flandrin G; Birnbaum D; Mozziconacci MJ; Lessard M Acute myeloid leukaemia with 8p11 (MYST3) rearrangement: an integrated cytologic, cytogenetic and molecular study by the groupe francophone de cytogenetique hematologique. *Leukemia* 2008, 22, 1567–1575. [PubMed: 18528428]
16. Lasko LM; Jakob CG; Edalji RP; Qiu W; Montgomery D; Digiammarino EL; Hansen TM; Risi RM; Frey R; Manaves V; Shaw B; Algire M; Hessler P; Lam LT; Uziel T; Faivre E; Ferguson D; Buchanan FG; Martin RL; Torrent M; Chiang GG; Karukurichi K; Langston JW; Weinert BT; Choudhary C; de Vries P; Van Drie JH; McElligott D; Kesicki E; Marmorstein R; Sun C; Cole PA; Rosenberg SH; Michaelides MR; Lai A; Bromberg KD Discovery of a selective catalytic p300/CBP inhibitor that targets lineage-specific tumours. *Nature* 2017, 550, 128–132. [PubMed: 28953875]
17. Lau OD; Kundu TK; Soccio RE; Ait-Si-Ali S; Khalil EM; Vassilev A; Wolffe AP; Nakatani Y; Roeder RG; Cole PA HATs off: selective synthetic inhibitors of the histone acetyltransferases p300 and PCAF. *Mol Cell* 2000, 5, 589–595. [PubMed: 10882143]
18. Kwie FH; Briet M; Soupaya D; Hoffmann P; Maturano M; Rodriguez F; Blonski C; Lherbet C; Baudoin-Dehoux C New potent bisubstrate inhibitors of histone acetyltransferase p300: design, synthesis and biological evaluation. *Chem Biol Drug Des* 2011, 77, 86–92. [PubMed: 21118378]
19. Bowers EM; Yan G; Mukherjee C; Orry A; Wang L; Holbert MA; Crump NT; Hazzalin CA; Liszczak G; Yuan H; Larocca C; Saldanha SA; Abagyan R; Sun Y; Meyers DJ; Marmorstein R;

- Mahadevan LC; Alani RM; Cole PA Virtual ligand screening of the p300/CBP histone acetyltransferase: identification of a selective small molecule inhibitor. *Chem Biol* 2010, 17, 471–482. [PubMed: 20534345]
20. Yang H; Pinello CE; Luo J; Li D; Wang Y; Zhao LY; Jahn SC; Saldanha SA; Chase P; Planck J; Geary KR; Ma H; Law BK; Roush WR; Hodder P; Liao D Small-molecule inhibitors of acetyltransferase p300 identified by high-throughput screening are potent anticancer agents. *Mol Cancer Ther* 2013, 12, 610–620. [PubMed: 23625935]
21. Costi R; Di Santo R; Artico M; Miele G; Valentini P; Novellino E; Cereseto A Cinnamoyl compounds as simple molecules that inhibit p300 histone acetyltransferase. *J Med Chem* 2007, 50, 1973–1977. [PubMed: 17348637]
22. Baell J; Walters MA Chemistry: Chemical con artists foil drug discovery. *Nature* 2014, 513, 481–483. [PubMed: 25254460]
23. Wu F; Zhou C; Yao Y; Wei L; Feng Z; Deng L; Song Y 3-(Piperidin-4-ylmethoxy)pyridine containing compounds are potent inhibitors of lysine specific demethylase 1. *J Med Chem* 2016, 59, 253–263. [PubMed: 26652247]
24. Pereira R; Furst A; Iglesias B; Germain P; Gronemeyer H; de Lera AR Insights into the mechanism of the site-selective sequential palladium-catalyzed cross-coupling reactions of dibromothiophenes/dibromothiazoles and arylboronic acids. Synthesis of PPARbeta/delta agonists. *Org Biomol Chem* 2006, 4, 4514–4525. [PubMed: 17268648]
25. Liu X; Wang L; Zhao K; Thompson PR; Hwang Y; Marmorstein R; Cole PA The structural basis of protein acetylation by the p300/CBP transcriptional coactivator. *Nature* 2008, 451, 846–850. [PubMed: 18273021]
26. Maksimoska J; Segura-Pena D; Cole PA; Marmorstein R Structure of the p300 histone acetyltransferase bound to acetyl-coenzyme A and its analogues. *Biochemistry* 2014, 53, 3415–3422. [PubMed: 24819397]
27. Demarest SJ; Martinez-Yamout M; Chung J; Chen H; Xu W; Dyson HJ; Evans RM; Wright PE Mutual synergistic folding in recruitment of CBP/p300 by p160 nuclear receptor coactivators. *Nature* 2002, 415, 549–553. [PubMed: 11823864]
28. Fu X; Jeselsohn R; Pereira R; Hollingsworth EF; Creighton CJ; Li F; Shea M; Nardone A; De Angelis C; Heiser LM; Anur P; Wang N; Grasso CS; Spellman PT; Griffith OL; Tsimelzon A; Gutierrez C; Huang S; Edwards DP; Trivedi MV; Rimawi MF; Lopez-Terrada D; Hilsenbeck SG; Gray JW; Brown M; Osborne CK; Schiff R FOXA1 overexpression mediates endocrine resistance by altering the ER transcriptome and IL-8 expression in ER-positive breast cancer. *Proc Natl Acad Sci U S A* 2016, 113, E6600–E6609. [PubMed: 27791031]
29. Morrison G; Fu X; Shea M; Nanda S; Giuliano M; Wang T; Klinowska T; Osborne CK; Rimawi MF; Schiff R Therapeutic potential of the dual EGFR/HER2 inhibitor AZD8931 in circumventing endocrine resistance. *Breast Cancer Res Treat* 2014, 144, 263–272. [PubMed: 24554387]
30. Ono H; Basson MD; Ito H P300 inhibition enhances gemcitabine-induced apoptosis of pancreatic cancer. *Oncotarget* 2016, 7, 51301–51310. [PubMed: 27322077]
31. Wang L; Gural A; Sun XJ; Zhao X; Perna F; Huang G; Hatlen MA; Vu L; Liu F; Xu H; Asai T; Deblasio T; Menendez S; Voza F; Jiang Y; Cole PA; Zhang J; Melnick A; Roeder RG; Nimer SD The leukemogenicity of AML1-ETO is dependent on site-specific lysine acetylation. *Science* 2011, 333, 765–769. [PubMed: 21764752]
32. Subramanian A; Tamayo P; Mootha VK; Mukherjee S; Ebert BL; Gillette MA; Paulovich A; Pomeroy SL; Golub TR; Lander ES; Mesirov JP Gene set enrichment analysis: A knowledge-based approach for interpreting genome-wide expression profiles. *Proceedings of the National Academy of Sciences* 2005, 102, 15545–15550.
33. Ianculescu I; Wu DY; Siegmund KD; Stallcup MR Selective roles for cAMP response element-binding protein binding protein and p300 protein as coregulators for androgen-regulated gene expression in advanced prostate cancer cells. *J Biol Chem* 2012, 287, 4000–4013. [PubMed: 22174411]
34. Jin Q; Yu LR; Wang L; Zhang Z; Kasper LH; Lee JE; Wang C; Brindle PK; Dent SY; Ge K Distinct roles of GCN5/PCAF-mediated H3K9ac and CBP/p300-mediated H3K18/27ac in nuclear receptor transactivation. *EMBO J* 2011, 30, 249–262. [PubMed: 21131905]

35. Zheng B; Yao Y; Liu Z; Deng L; Anglin JL; Jiang H; Prasad BV; Song Y Crystallographic investigation and selective inhibition of mutant isocitrate dehydrogenase. *ACS Med Chem Lett* 2013, 4, 542–546. [PubMed: 23795241]
36. Wu F; Jiang H; Zheng B; Kogiso M; Yao Y; Zhou C; Li XN; Song Y Inhibition of cancer-associated mutant isocitrate dehydrogenases by 2-thiohydantoin compounds. *J Med Chem* 2015, 58, 6899–6908. [PubMed: 26280302]
37. Feng Z; Yao Y; Zhou C; Chen F; Wu F; Wei L; Liu W; Dong S; Redell M; Mo Q; Song Y Pharmacological inhibition of LSD1 for the treatment of MLL-rearranged leukemia. *J Hematol Oncol* 2016, 9:24. [PubMed: 26970896]
38. Zhang L; Deng L; Chen F; Yao Y; Wu B; Wei L; Mo Q; Song Y Inhibition of histone H3K79 methylation selectively inhibits proliferation, self-renewal and metastatic potential of breast cancer. *Oncotarget* 2014, 5, 10665–10677. [PubMed: 25359765]
39. Martin M Cutadapt removes adapter sequences from high-throughput sequencing reads. 2011, 17, 3.
40. Andrews S FastQC A quality control tool for high throughput sequence data. <http://www.bioinformatics.babraham.ac.uk/projects/fastqc/>. (accessed March 27, 2018).
41. Perteau M; Kim D; Perteau GM; Leek JT; Salzberg SL Transcript-level expression analysis of RNA-seq experiments with HISAT, StringTie and Ballgown. *Nat Protoc* 2016, 11, 1650–1667. [PubMed: 27560171]
42. Li H; Handsaker B; Wysoker A; Fennell T; Ruan J; Homer N; Marth G; Abecasis G; Durbin R The sequence alignment/map format and SAMtools. *Bioinformatics* 2009, 25, 2078–2079. [PubMed: 19505943]

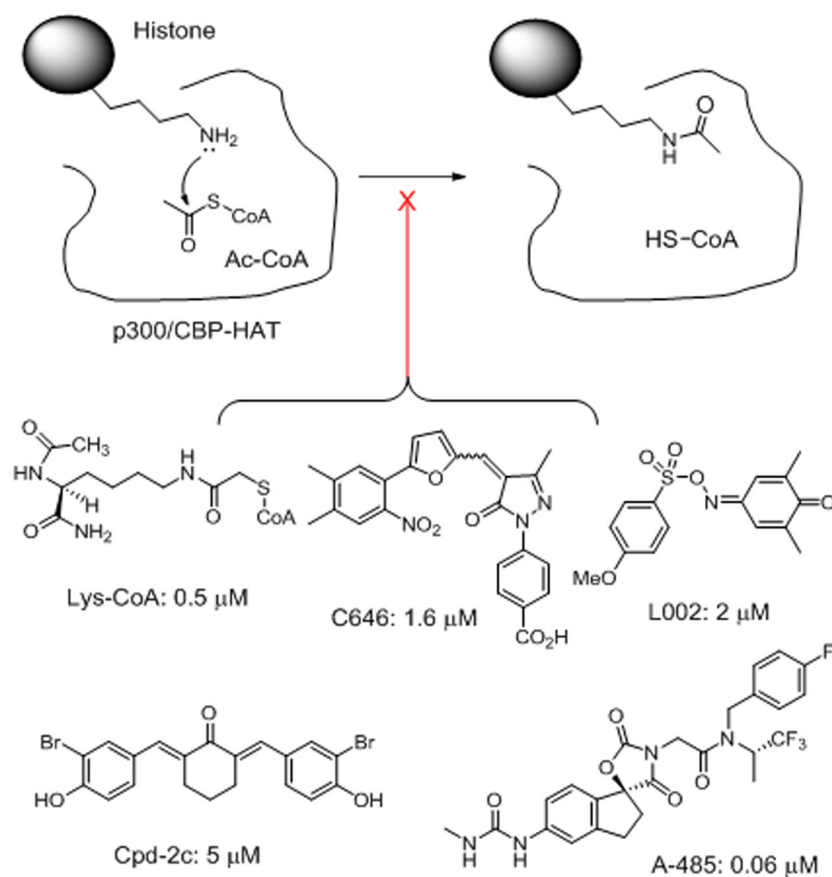


Figure 1. P300/CBP HAT catalyzed reaction and inhibitors with their IC₅₀ values.

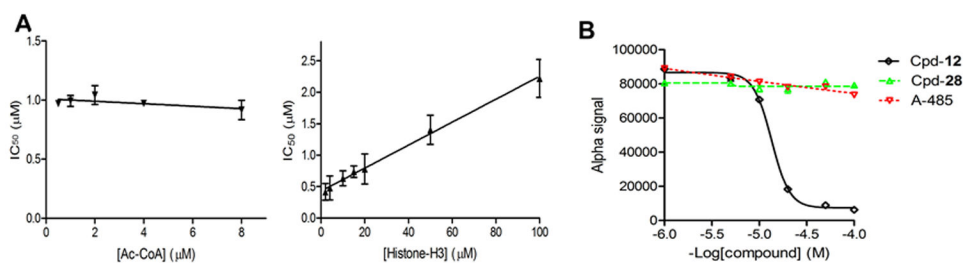


Figure 2.

Compound **12** is a competitive inhibitor of p300 HAT against the substrate histone. (A) Plots of IC₅₀ values of **12** versus increasing concentrations of (left) Ac-CoA (0.5 - 8 μM, or 0.07-1.2× K_m) and (right) histone H3 suggest the inhibitor is non-competitive against Ac-CoA and competitive against histone; (B) Alpha assay results show compound **12** can dose-dependently disrupt the binding between p300 HAT and histone H4. But such binding was not affected by inactive compound **28** as well as A-485 which is an inhibitor competitive against Ac-CoA.

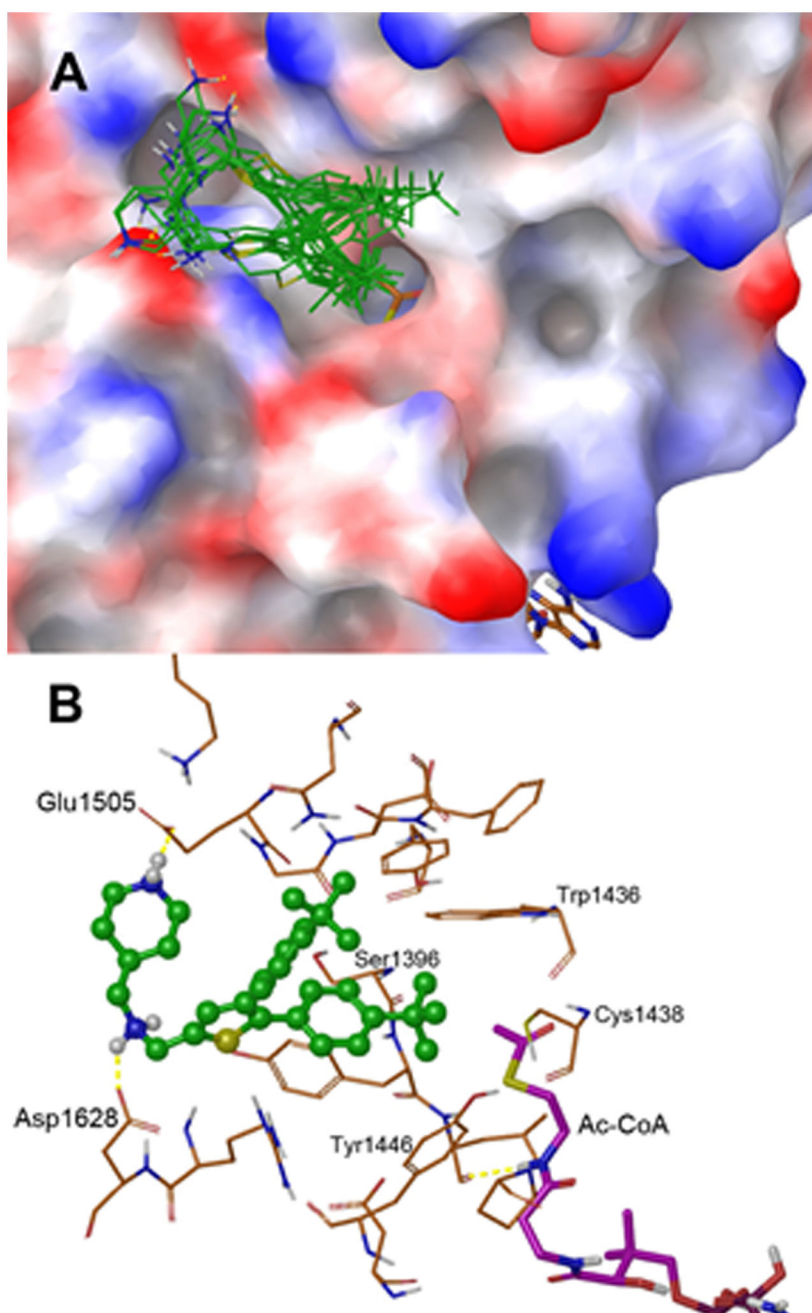


Figure 3. Docking results for compound **12**. (A) 10 docking conformations of **12** (with C atoms in green) with lowest energies in the crystal structure of p300-HAT (PDB: 4PZS, shown as an electrostatic surface) in complex with Ac-CoA (as a tube model with C atoms in brown); and (B) The lowest energy docking conformation of **12** (as a ball-and-stick model) with surrounding residues and Ac-CoA in p300-HAT (PDB: 4PZS). Hydrogen bonds are shown as yellow dotted lines.

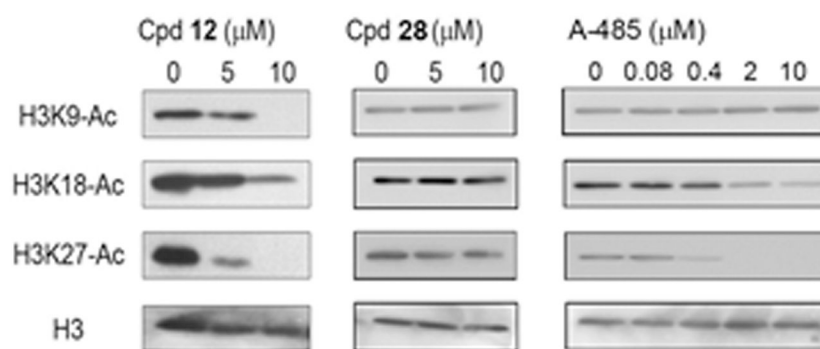


Figure 4. Cellular activity of compounds **12**, **28** and A-485 against acetylation of H3K9, H3K18 and H3K27.

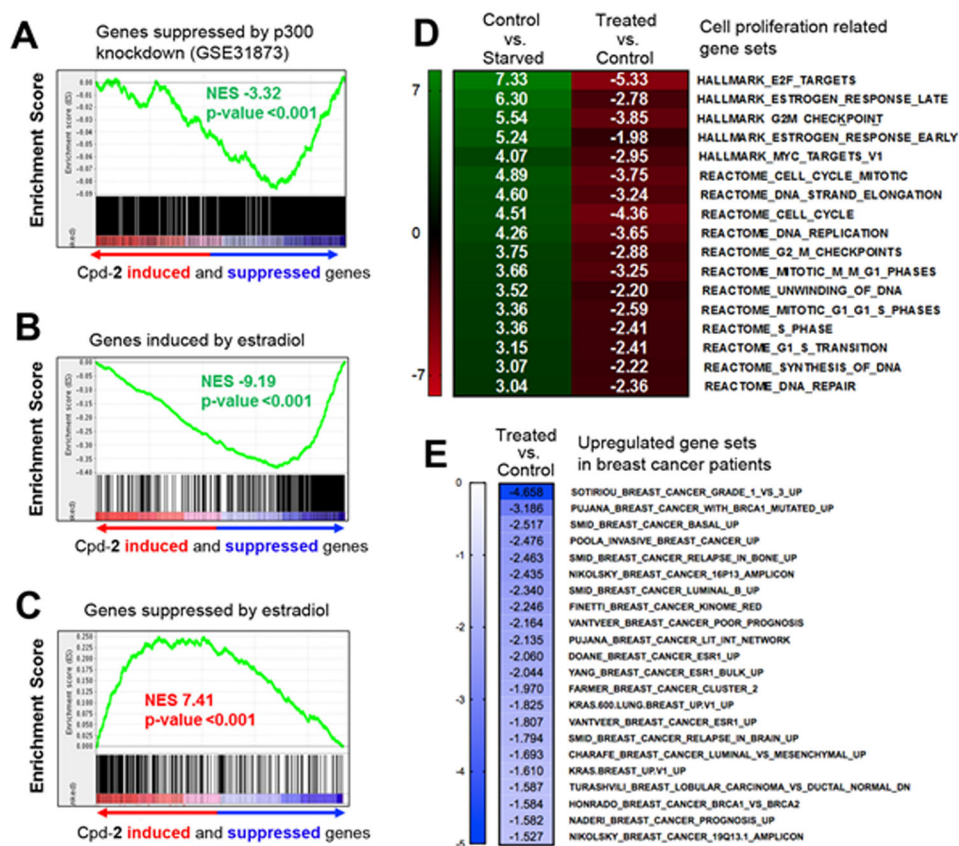


Figure 5. Gene set enrichment analysis (GSEA) results showing significant gene expression changes ($p < 0.001$) in ER+ MCF-7 cells by treatment with p300 HAT inhibitor **12**, as compared to the starved (without estradiol) or control (with estradiol) group. (A) Inhibitor treatment caused significant downregulation of genes that were suppressed by siRNA-mediated p300 knockdown (GSE31873); (B-D) Results showing compound **12** counteracted estradiol in MCF-7 cells. Treatment with **12** significantly (B) suppressed expression of genes that were upregulated by estradiol, and (C) induced expression of genes that were downregulated by estradiol. (D, E) GSEA heatmaps of normalized enrichment scores (NES) for publicly available gene signatures (from the MSigDB database). (D) Inhibitor **12** caused significant downregulation of cancer-related gene sets that were induced by estradiol; (E) Inhibitor **12** suppressed expression of gene sets associated with breast cancer as well as the poor prognosis, progression, invasion and relapse of breast cancer.

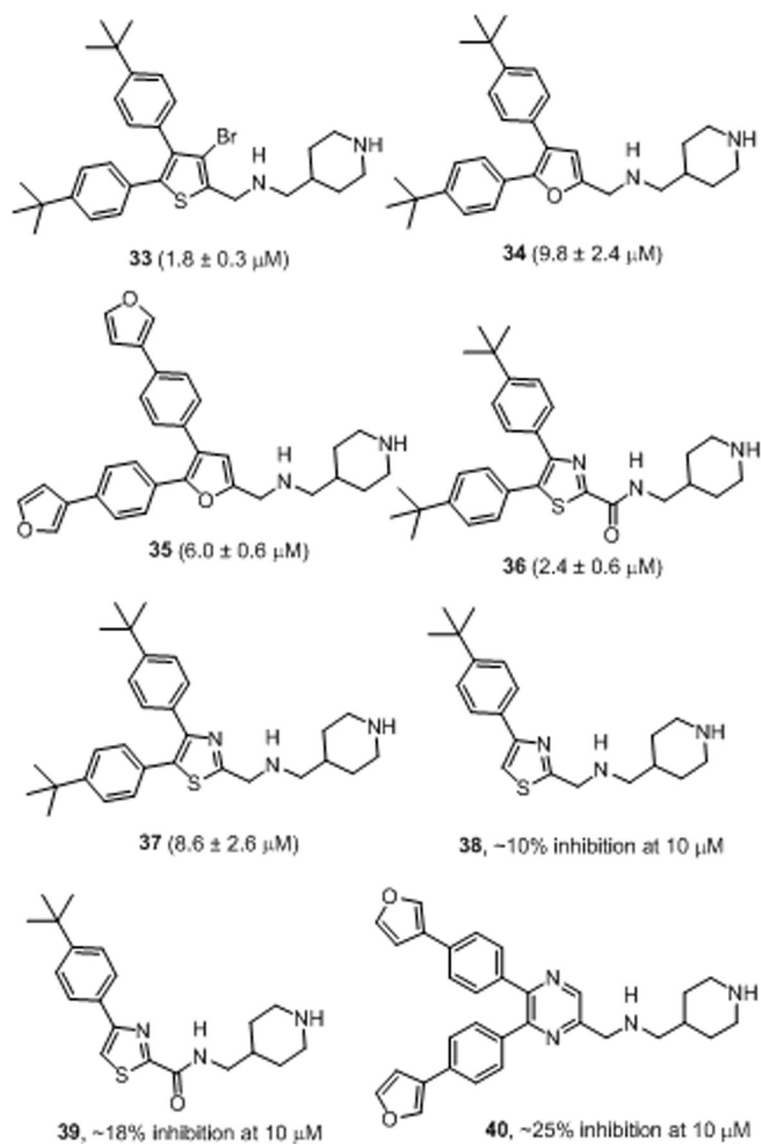
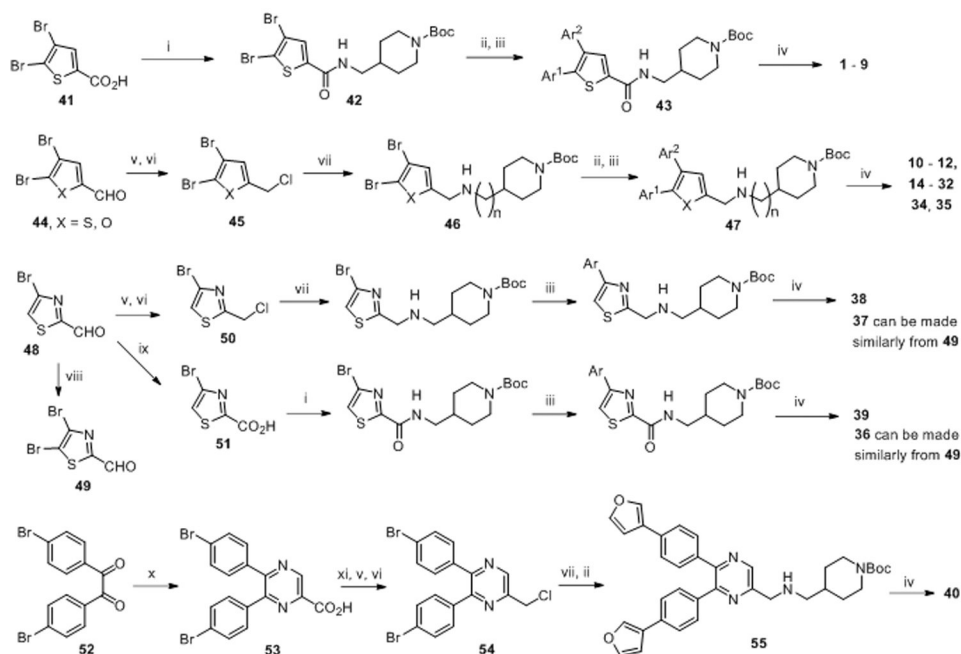


Chart 1.
Structures and inhibitory activity of compounds 33-40.



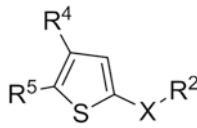
Scheme 1.

General synthetic methods for thiophene-containing compounds.^a

^a *Reagents and conditions:* (i) 1-ethyl-3-(3-dimethylaminopropyl)carbodiimide, 1-hydroxybenzotriazole, 4-(aminomethyl)-1-BOC-piperidine, CH₂Cl₂, 96% yield; (ii) Ar¹-B(OH)₂, Pd(PPh₃)₄, Na₂CO₃, 80 °C, 80-90% yield; (iii) Ar²-B(OH)₂, Pd(PPh₃)₄, Na₂CO₃, 100 °C, 80-90% yield; (iv) HCl in 1,4-dioxane, >90% yield; (v) NaBH₄, MeOH; (vi) cyanuric chloride, DMF, 81% yield for the 2 steps; (vii) 4-(aminomethyl)-1-BOC-piperidine or other amine analogs, K₂CO₃, DMF, 60-85% yield; (viii) N-Bromosuccinimide, CH₂Cl₂; (ix) NaClO₂, NaH₂PO₄, *tert*-butanol-H₂O, 2-methyl-2-butene; (x) 2,3-diaminopropanoic acid, NaOH, MeOH, reflux, 55% yield; (xi) ClCO₂Me, (*i*Pr)₂NEt, THF, 95% yield.

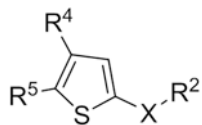
Table 1.

Structure and inhibitory activity of compounds 1-32.



The chemical structure shows a thiophene ring with a sulfur atom at the bottom. The 2-position is substituted with R⁴, the 3-position with R⁵, and the 4-position with an X-R² group.

Cpd	R ⁴	R ⁵	X	R ²	IC ₅₀ (μM) (% inhibition at 10 μM)
1	4- <i>t</i> -Bu-Ph	= R ⁴	-CONH-	piperidin-4-ylmethyl	8.6 ± 0.4
2	4-(furan-3-yl)-Ph	= R ⁴	-CONH-	same as above	1.6 ± 0.2
3	4-methoxybiphenyl	= R ⁴	-CONH-	same as above	2.8 ± 0.6
4	4-(furan-3-yl)-Ph	4- <i>t</i> -Bu-Ph	-CONH-	same as above	7.4 ± 0.8
5	4-aminomethyl-Ph	4- <i>t</i> -Bu-Ph	-CONH-	same as above	10.0 ± 1.4
6	4-(piperidin-1-ylmethyl)-Ph	4-(furan-3-yl)-Ph	-CONH-	same as above	1.6 ± 0.2
7	4-(piperazin-1-ylmethyl)-Ph	4- <i>t</i> -Bu-Ph	-CONH-	same as above	>10 (12%)
8	furan-3-yl	4- <i>t</i> -Bu-Ph	-CONH-	same as above	>10 (36%)
9	pyridin-3-yl	4- <i>t</i> -Bu-Ph	-CONH-	same as above	>10 (31%)
10	4-methoxybiphenyl	= R ⁴	-CH ₂ NH-	same as above	7.4 ± 1.0
11	4-(furan-3-yl)-Ph	= R ⁴	-CH ₂ NH-	same as above	1.7 ± 0.2
12	4- <i>t</i> -Bu-Ph	= R ⁴	-CH ₂ NH-	same as above	0.62 ± 0.2
13	4- <i>t</i> -Bu-Ph	= R ⁴	-CH ₂ O-	same as above	>10 (0%)
14	4- <i>t</i> -Bu-Ph	= R ⁴	-CH ₂ NH-	piperidin-4-yl	5.0 ± 1.6
15	4- <i>t</i> -Bu-Ph	= R ⁴	-CH ₂ NH-	2-(piperidin-4-yl)ethyl	2.2 ± 0.4
16	4- <i>t</i> -Bu-Ph	= R ⁴	-CH ₂ NH-	3-aminopropyl	3.0 ± 1.0
17	4- <i>t</i> -Bu-Ph	= R ⁴	-CH ₂ NH-	6-aminoethyl	1.4 ± 0.3
18	4- <i>t</i> -Bu-Ph	= R ⁴	-CH ₂ -	piperazin-1-yl	>10 (5%)
19	4- <i>t</i> -Bu-Ph	= R ⁴	-CH ₂ -	morpholin-4-yl	>10 (20%)
20	4- <i>t</i> -Bu-Ph	= R ⁴	-CH ₂ N(Me)-	piperidin-4-ylmethyl	4.4 ± 1.6
21	4- <i>t</i> -Bu-Ph	= R ⁴	-CH ₂ N(CHO)-	same as above	7.0 ± 1.6
22	4- <i>t</i> -Pr-Ph	= R ⁴	-CH ₂ NH-	same as above	5.4 ± 1.4
23	4-Bu-Ph	= R ⁴	-CH ₂ NH-	same as above	>10 (10%)
24	4-(furan-3-yl)-Ph	4- <i>t</i> -Bu-Ph	-CH ₂ NH-	same as above	5.8 ± 0.6
25	4-(furan-3-yl)-Ph	4-(piperidin-1-ylmethyl)-Ph	-CH ₂ NH-	same as above	4.6 ± 1.4
26	4- <i>t</i> -Bu-Ph	4-aminomethyl-Ph	-CH ₂ NH-	same as above	2.0 ± 0.5
27	4-aminomethyl-Ph	4- <i>t</i> -Bu-Ph	-CH ₂ NH-	same as above	>10 (35%)
28	4-aminomethyl-Ph	= R ⁴	-CH ₂ NH-	same as above	>10 (0%)
29	4-hydroxymethyl-Ph	= R ⁴	-CH ₂ NH-	same as above	>10 (22%)
30	furan-3-yl	= R ⁴	-CH ₂ NH-	same as above	>10 (23%)



Cpd	R ⁴	R ⁵	X	R ²	IC ₅₀ (μM) (% inhibition at 10 μM)
31	3,4-dimethoxy-Ph	= R ⁴	-CH ₂ NH-	same as above	>10 (0%)
32	3-biphenyl	= R ⁴	-CH ₂ NH-	same as above	>10 (18%)

Table 2.Inhibitory activities of compound **12** against HATs.

	IC₅₀ (μM)
P300-HAT	0.62 ± 0.12
CBP-HAT	1.2 ± 0.13
PCAF	>50
Myst3	>50

Author Manuscript

Author Manuscript

Author Manuscript

Author Manuscript

Table 3.Antiproliferative activity EC₅₀ (μM) of compounds **12**, **28**, **31** and A-485.

	Cpd-12	Cpd-28	Cpd-31	A-485
MCF-7	2.8 ± 0.1	>30	>30	>30
MCF-7 (Tam-R)	3.4 ± 0.1	>30	>30	>30
PANC-1	1.0 ± 0.2	>30	>30	>30
MDA-PANC-28	2.8 ± 0.4	>30	>30	>30
Kasumi-1	2.6 ± 0.6	>30	18.7 ± 0.1	0.33 ± 0.01

Author Manuscript

Author Manuscript

Author Manuscript

Author Manuscript